FUNCTIONAL CHARACTERIZATION OF BREVETOXIN-INDUCED NEUROTOXICITY

IN CORTICAL NEURONS USING MEMBRANE POTENTIAL-SENSITIVE

FLUORESCENT PROBES AND CELL SIGNALING ASSAYS

by

JENNIFER HILL-HOFFMAN PETERSON

(Under the Direction of Thomas F. Murray)

ABSTRACT

Brevetoxins represent a series of structurally related polyether neurotoxins that have been implicated in numerous epizootics and human exposures worldwide. Brevetoxins exert their effects by binding to voltage-gated sodium channels in the brain and altering their gating properties resulting in the propagation of continuous action potentials and the subsequent overactivation of N-methyl-D-aspartate receptors (NMDAR) in neurons. After optimizing assay conditions for the two membrane potential-sensitive fluorescent dyes $DiBAC_4(3)$ and the Membrane Potential Assay Kit (FMPblue, Molecular Devices Inc., blue dye) in intact neurons, we developed standard conditions that allowed us to quantify the magnitude of PbTx-2-induced depolarization through comparison to that produced by KCl in neocortical cells. We found that 300 nM PbTx-2 and 15 mM KCl produce equivalent levels of membrane potential in neocortical cells. Using this data, we determined that both $[Na^+]_i$ and Src tyrosine kinase are involved in PbTx-2-induced upregulation of NMDARs.

INDEX WORDS: brevetoxin, red tide, NMDA receptor, Membrane Potential-Sensitive
                 Fluorescent Dyes, voltage-gated sodium channel, neocortical neurons

FUNCTIONAL CHARACTERIZATION OF BREVETOXIN-INDUCED NEUROTOXICITY

IN CORTICAL NEURONS USING MEMBRANE POTENTIAL-SENSITIVE

FLUORESCENT PROBES AND CELL SIGNALING ASSAYS

by

JENNIFER HILL-HOFFMAN PETERSON

B.S.A., The University of Georgia, 2003

A Thesis Submitted to the Graduate Faculty of The University of Georgia in Partial Fulfillment

of the Requirements for the Degree

MASTER OF SCIENCE

ATHENS, GEORGIA

2005

FUNCTIONAL CHARACTERIZATION OF BREVETOXIN-INDUCED NEUROTOXICITY

IN CORTICAL NEURONS USING MEMBRANE POTENTIAL-SENSITIVE

FLUORESCENT PROBES AND CELL SIGNALING ASSAYS

by

JENNIFER HILL-HOFFMAN PETERSON

Major Professor: Thomas F. Murray

Committee: Raghubir P. Sharma
                     Frederick D. Quinn

DEDICATION

This thesis is dedicated to my family who has taught me how to pursue my

dreams relentlessly and my husband who has stood by, encouraged, and loved me unselfishly.

He has been my rock the entire way. I love you all so much.

ACKNOWLEDGEMENTS

TABLE OF CONTENTS

LIST OF TABLES

LIST OF FIGURES

CHAPTER 1

INTRODUCTION AND REVIEW OF THE LITERATURE

INTRODUCTION

Marine dinoflagellates are becoming more and more of a concern among the coastal population as their impact has continued to grow and spread through the years [5,8]. Dinoflagellates are single-celled planktonic animals that have the ability to produce toxins resulting in a negative affect on surrounding wildlife. The danger of these dinoflagellates at normal levels is low, however, various triggering factors can result in explosive growth of the algae and a subsequent significant increase in toxin production. Due to the toxin's involvement in the deaths of thousands of marine animals and toxicity in humans, they have received added attention in recent years. A toxin of particular concern in the Gulf of Mexico and recently off the coasts of New Zealand and Japan is known as brevetoxin [3,23]. Brevetoxins represent a series of structurally related polyether neurotoxins produced by the dinoflagellate *Karenia brevis* (formerly *Gymnodinium breve* and *Ptychodiscus brevis*). This dinoflagellate is known for its involvement in the 'red tide,' a yearly phenomenon named appropriately for the apparent red coloring of surrounding water due to its explosive growth and spreading among oceanic waters.

EPIDEMIOLOGY

Brevetoxin has been implicated in numerous epizootics including an outbreak off the coast of Florida in 1996, where 149 manatees were found dead or dying along Florida's coastline and a Texas bloom in 1997 killing over 14 million fish [8]. The Manatees were found with severe nasopharyngeal, pulmonary, hepatic, renal, and cerebral congestion along with edema in the nasopharyngeal and pulmonary regions. Brevetoxin was suggested to initiate apoptosis following its accumulation leading to the release of inflammatory cytokines that culminate fatal toxic shock [9]. A more recent investigation has occurred involving an "Unusual Mortality

2

Event" (UME) linked to a red tide that occurred during March/April of 2004 where approximately 100 bottlenose dolphins were found stranded dead along the Florida Panhandle in addition to hundreds of fish and marine invertebrates [1].

Brevetoxins (PbTx) exist in forms 1-10, with PbTx-2 being the primary toxin produced [35]. Red tides are characteristic of *Karenia brevis* outbreaks where the red alga comes dangerously close to the shore. Brevetoxin is excreted and released into the water upon algal cell rupture by the ocean's beating currents. These toxins can then either affect surrounding marine wildlife or undergo bubble-mediated transport to the surface where they are released into the air and incorporated into marine aerosol [33,35]. Inhalation of aerosolized brevetoxin can cause Respiratory Irritation Syndrome, characterized by conjuctival irritation, rhinorrhea, and nonproductive cough in individuals in close proximity to the infested waters. Persons swimming in red tide waters have been reported to experience eye and skin irritation and itching sensations [16]. Shellfish poisoning has been a common route of toxicosis due to the ability of the toxin to accumulate in the tissue of bivalves as water is swept through their gills. Consumption of contaminated shellfish results in Neurotoxic Shellfish Poisoning (NSP), a syndrome characterized by paresthesia, reversal of temperature sensation, vertigo, ataxia, and myalgia. Other symptoms include gastrointestinal disorders causing severe abdominal pain, nausea, and diarrhea [29]. Developmental abnormalities have been observed in fish after having been exposed via microinjection of PbTx directly into the egg. Consequences of exposure included impaired hatching success and larvae survival where those that did survive demonstrated excessive tail and body twitching in early stages of development with curvature of the spine resulting in the inability to swim well enough to survive [10].

Karenia brevis cultures, normally maintained around 1,000 cells/L throughout the year, can reach levels of 100,000 cells/L during a red tide event [42]. The impact of these toxin-producing cells on surrounding resources has been approximated to reach a 15-year loss of over $400 million and has initiated over 600,000 individual cases of human intoxication annually in the US alone [5]. These data suggest the astronomical effects that brevetoxin has on the economy and on human health and thus, underline the importance for concern and action in improving the outcome of PbTx exposure.

STRUCTURE, METABOLISM, AND EXCRETION

The basic structure of brevetoxin exists as a polyether planar molecule with eleven transfused rings, 23 stereocenters and an overall linear low-energy conformation [24] (Fig. 1.1). Two structural backbone types are known to exist and are labeled as type A and type B, each with variations in the R group attached to ring J or K, respectively [36]. The eleven transfused rings consist of one lactone, labeled as the A-lactone ring and representing the 'head' region of the chain, with ten ether rings labeled as H-K and representing the 'tail' region. Type A brevetoxins, PbTx-1, 7, and 10, have been found to be more potent than type B due to destruction of hydrophobic character, however, they are relatively unstable and of limited supply [34]. Type B brevetoxins, PbTx-2, 3, 9, and 8, are much more stable maintaining structure up to 300°C and will remain potent for months when stored properly [34].

Out of the type B brevetoxins, PbTx-2 is the major naturally occurring brevetoxin produced with successively lower amounts of PbTx-3 and PbTx-1. During the log phase of growth, *Kerenia brevis* produces these toxins in the approximate ratio of 20:4:1, respectively [35]. During dispositional studies following brevetoxin exposure, however, PbTx-3 has been

4

found to be the major brevetoxin present suggesting either the metabolic conversion of PbTx-2 to

PbTx-3 or a higher metabolic stability and preferential preservation for PbTx-3, although the

later is thought to be unlikely [35]. It is possible that the metabolic conversion of PbTx-2 to

PbTx-3 exists as the first step in producing conjugated phase-2 metabolites in physiological

detoxification processes inasmuch as PbTx-3 contains various metabolic conversion sites such as

the primary alcohol, K-ring, or the double bond associated with the eight-membered H-ring.

The hydrophobicity of PbTx's structure allows it to be rapidly cleared from the blood and

lungs and concentrate in lipid-rich tissues such the brain [43,45]. The major route of excretion

has been found to be the liver and bile [45].

Brevetoxin B backbone

Brevetoxin A backbone

Brevetoxin B backbone, R =
PbTx-2, $CH_2C(=CH_2)CHO$
PbTx-3, $CH_2C(=CH_2)CH_2OH$
PbTx-5, [PbTx-2], C-37 OAc
PbTx-6, [PbTx-2], H-ring epoxide
PbTx-8*, CH_2COCH_2Cl
PbTx-9, $CH_2CH(CH_3)CH_2OH$

Brevetoxin A backbone, R =
PbTx-1, $CH_2C(=CH_2)CHO$
PbTx-7, $CH_2C(=CH_2)CH_2OH$
PbTx-10, $CH_2CH(CH_3)CH_2OH$
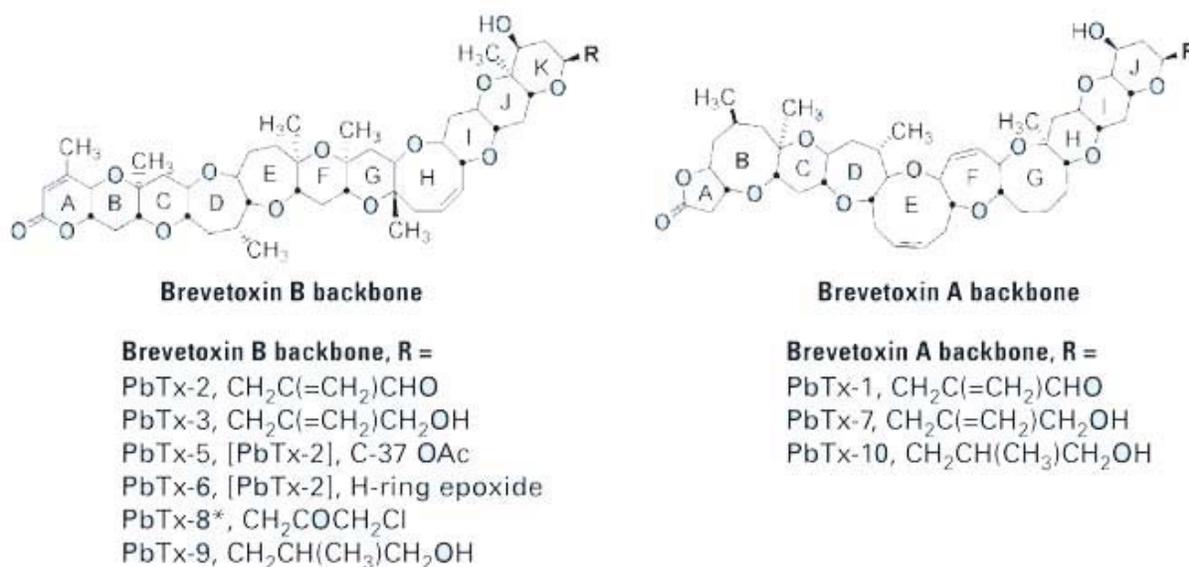
Figure 1.1. *The structures of brevetoxin* [4].

VOLTAGE-GATED SODIUM CHANNELS (VGSC)

VGSCs are responsible for the initiation and propagation of action potentials in excitable tissues and therefore represent essential entities in cell-to-cell communication and normal physiological function [30]. Hodgkin and Huxley were the first to characterize VGSCs using traditional patch clamp techniques identifying their key features as exhibiting voltage-dependent activation, rapid inactivation, and selective ion conductance to sodium [21]. Today, VGSCs are thought to exist in the mammalian brain as a dimeric structure with one large alpha subunit and two smaller beta subunits, namely beta1 and beta2. The alpha subunit of the channel is vital to receptor function inasmuch as it contains all of the channels major properties and has the ability to single-handedly form a functional channel [46]. The beta subunit, however, has been found to have functional roles in channel stability, glycosylation, modulation of channel inactivation kinetics, and neural cell-adhesion [15]. The VGSC consists of four domains (DI-IV) each with six alpha-helical transmembrane segments (S1-6) (Fig. 1.2). Both the amino- and carboxy- end are located intracellularly and aid as phosphorylation and glycosylation sites for channel modulation. The 6 transmembrane segments are connected via 3 intracellular loops, which also function in the overall activity of the channel including modulation of channel kinetics and channel inactivation [12]. The voltage-dependent activation of the channel is derived from the 'voltage-sensing' S4 segments located within each domain. These segments contain repeated motifs consisting of a positively charged amino acid residue followed by two hydrophobic residues. These motifs form a ribbon of positive charge that spirals around the cylindrical alpha helix and forms a type of voltage-sensitive door. Two models of this sensor conformation that have received added support over the years are the sliding helix [11] and helical screw models [18].
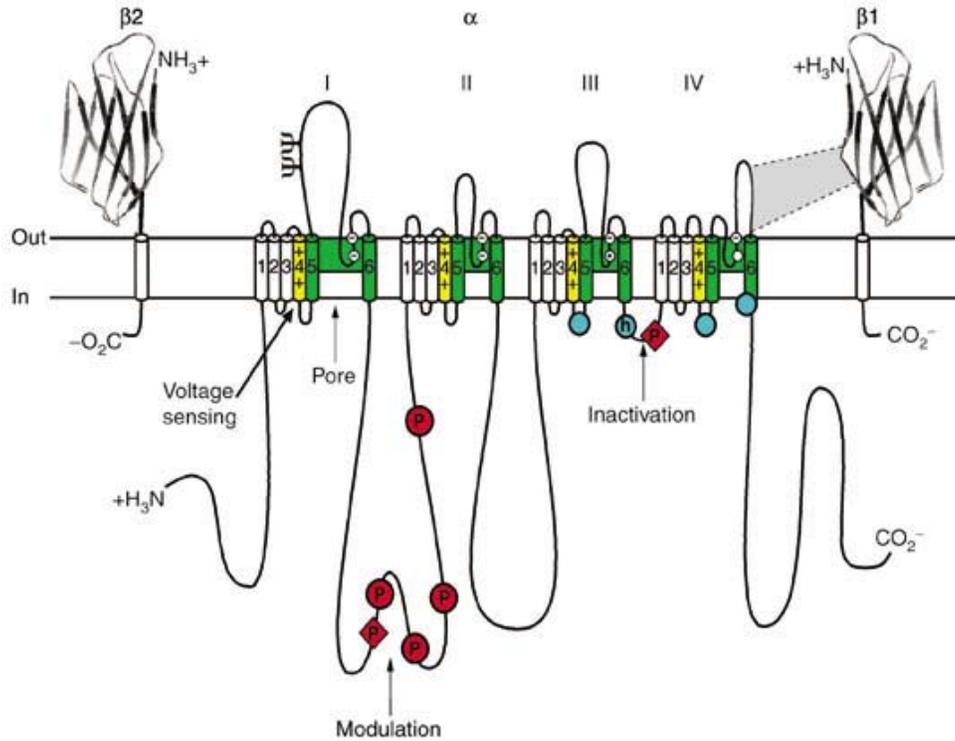
Figure 1.2. *The voltage-gated sodium channel* [48].

BREVETOXIN BINDING TO VGSCs

Gawley and Baden (1995) have previously described Brevetoxins' binding to VGSCs in detail. In general, the toxin binds the open conformation of the channel at neurotoxin binding site 5 in a head down orientation near the interface of domains I and IV, thereby, obstructing the normal motion of the IFM motif [3,17,24] (Fig. 1.3). The IFM motif is named for the succession of the three amino acid residues isoleucine, phenylalanine, and methionine located within the cytoplasmic loop between domains III and IV. This motif is thought to act as a 'plug' required to achieve inactivation of the channel [12]. Furthermore, an immobilization of S6 segments of the channel results from the relative stability of the A-ring of the toxin, which acts as a hydrogen bond acceptor and induces longer mean open times [17]. In summary, brevetoxin's ability to

bind in this way results in the toxin's ability to shift the membrane potential to more negative values, inhibit inactivation, and increase channel mean open time thereby effecting the excitability of nerve, muscle, and cardiac tissues [36,46].
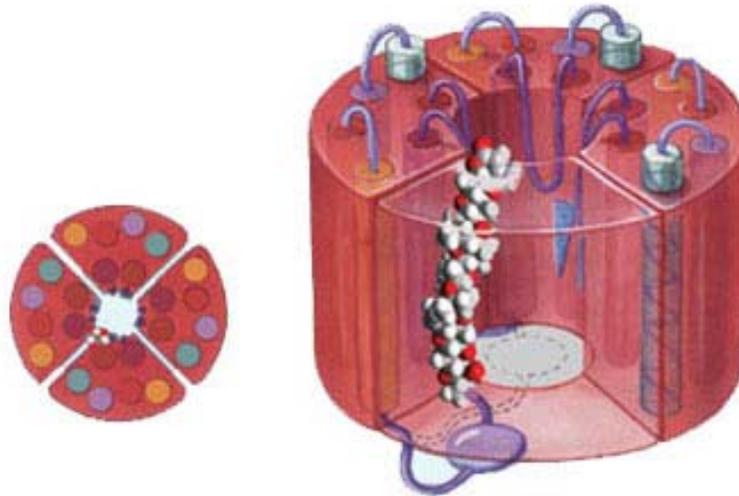
Figure 1.3. *Brevetoxin binding to VGSCs* [4].

GLUTAMATE AND THE NMDA RECEPTOR

Neurotransmitters can be defined as chemical "messengers" that are released during nerve impulses and transmit signals from one nerve cell to another. Glutamate is the primary neurotransmitter produced in the mammalian central nervous system and therefore plays a very large role in many of the brains physiological processes. Glutamate, once released into the synaptic space, binds to glutamate receptors on postsynaptic neurons to initiate a variety of cellular events eventually leading to cell function and viability. A glutamate receptor that has received an increasingly large amount of support over the years is the *N*-methyl-D-aspartate

receptor (NMDAR), named for its ability to bind and become activated by *N*-methyl-D-aspartate [28,47]. NMDARs are thought to be key players in synaptic plasticity leading to changes in neuronal development, and learning and memory. Furthermore, these receptors represent major therapeutic targets in such neurological and psychiatric disorders including epilepsy, amnesia, motor neuron disease, stroke, anxiety and psychosis as well as common neurodegenerative diseases such as Huntington's, Parkinson's, and Alzheimer's [27,37].

NMDARs are heteroligameric complexes that exist in mammalian systems as either tetramers or pentamers and are usually composed of one NR1 subunit and one or more of four NR2 subunits, namely NR2A-D. Highly active channels exist primarily when there is a NR1 subunit expressed together with at least one NR2 subunit.

The NMDAR is a unique receptor inasmuch as it possesses a multiplicity of activation mechanisms that must occur synonymously for its normal function. These mechanisms are thought to include the binding of the ligands, glutamate and the coagonist, glycine [20], to the receptor as well as the removal of a voltage-dependent Mg^{2+} block located within the channel pore [26]. Other factors that are thought to influence the channel kinetics include various phosphorylation and glycosylation events. Src is a protein tyrosine kinase abundantly expressed in the CNS and is thought to be involved in the phosphorylation of NMDARs and subsequent upregulation of channel function [38]. However, these mechanisms still remain partially enigmatic and therefore require further exploration as to possible mechanisms involved.

NMDARs are also unique in that they are highly permeable to Ca^{2+} ions and are therefore linked to signaling cascades that control cell survival making them important yet dangerous if disrupted. In a review on NMDAR signaling, Hardingham and Bading discuss the "Jekyll and Hyde" behavior that makes these receptors so interesting as their existence is vital yet potentially

harmful to a cell [19]. Furthermore, this fate in cell viability has more recently been proposed to be controlled by the location, synaptic or extrasynaptic, of the NMDAR [44]. These differences in structure and pharmacology of NMDARs may possibly provide a method of exploitation in the future for the development of treatments for neurodegenerative conditions involving these receptors.

BREVETOXIN-INDUCED EXCITOTOXICITY

Brevetoxin, due to its ability to initiate repetitive action potentials and cause a build-up of glutamate in the synaptic cleft of effected nerve fiber connections leads to subsequent excitotoxicity in nerve cells [7]. Excitotoxicity is a term originally coined by Olney referring to the toxic effects that stream from a cell overexcited by abnormal levels of an excitatory amino acid such as glutamate [31]. In other words, glutamate build-up in the synaptic cleft can lead to an overactivation of NMDARs and increase intracellular Ca^{2+} levels to those which are considered deadly to cells. Ca^{2+} levels inside a cell are restricted to very finite levels (~100nM) and if disrupted can lead to the initiation of a variety of enzymatic pathways and cascade-like effects including the overactivation of proteases, lipases, endonucleases, and phosphatases eventually leading either directly to damage in cell structure or indirectly to cell death through the formation of oxidative free radicals [2,40]. Of coarse, as discussed earlier, Ca^{2+} influx through NMDARs may lead to signaling cascades that are more likely to end in these types of mechanisms indicating why brevetoxin is so toxic to cells [7,39].

THE MITOGEN-ACTIVATED PROTEIN KINASE (MAPK) CASCADE

MAPKs form a family of protein kinase cascades which represent important intermediates in signal transduction pathways that control such vital processes as cell differentiation, proliferation, and death [32]. These cascades are thought to be activated by various mechanisms, which allow for the integration of diverse signals from both intracellular and extracellular environments that will ultimately direct the cells response to proliferative cues or stressful stimuli [41]. These mechanisms include activation of, as well as the interaction between, G protein-coupled receptors (GPCR), receptor protein tyrosine kinases (RPTK), and various 2nd messenger systems [6,13,14].

Three well-characterized subfamilies of MAPKs are extracellular signal-regulated protein kinase 1 and 2 (ERK1/2), c-JUN NH2-terminal protein kinase (JNK)/stress-activated protein kinase (SAPK), and p-38. These MAPKs are thought to play different roles in many cellular activities, possibly maintaining those opposing one another in cell viability [25]. Of the three subfamilies, the ERK1/2 pathway is thought to be the best understood and has been proposed to participate in many fundamental cellular processes including proliferation, differentiation, growth, survival, and apoptosis [6,41]. One mechanism of ERK1/2 activation has been established to exist through RPTK coupling via a growth factor receptor bound protein-2 (GRB2)-Ras guanonucleotide exchange protein SOS-Ras-Raf-mitogen-activated, extracellular signal-regulated protein kinase kinase (MEK) connection (Fig. 1.4). In short, GRB2-SOS complex translocation to the plasma membrane upon autophosphorylation through RPTK results in activation of the G-protein Ras. Ras then activates the MAPK kinase kinase, Raf, which in turn activates the MAPK kinase, MEK1/2 (MAP/ERK1/2 kinase), and finally activates the

MAPK, ERK1/2. ERK1/2 may then enter into the nucleus and activate various transcription

factors ultimately determining the fate of the cell [22].
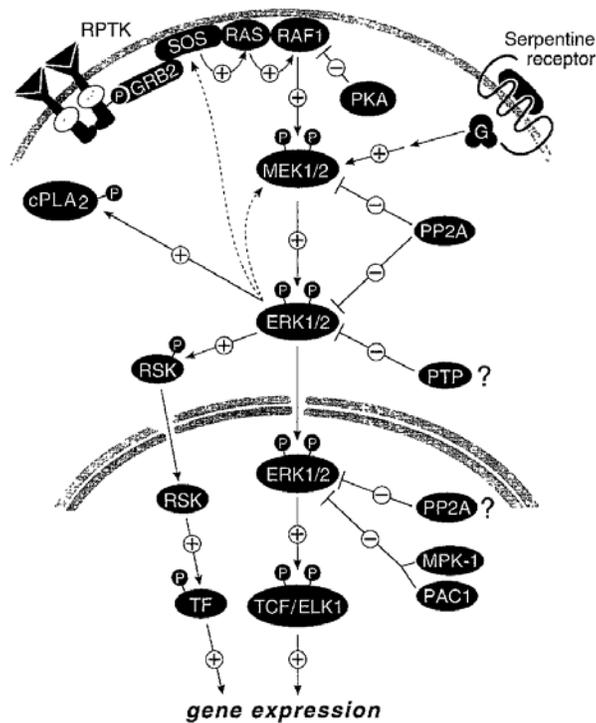
Figure 1.4. *The ERK1/2 MAPK Pathway* [22].

REFERENCES

[1]   Interim Report on the Bottlenose Dolphin (Tursiops truncatus) Unusual Mortality Event

        Along the Panhandle of Florida., National Oceanic and Atmospheric Administration:

        U.S. Department of Commerce, 2004.

[2]   Atlante, A., Calissano, P., Bobba, A., Giannattasio, S., Marra, E. and Passarella, S.,

        Glutamate neurotoxicity, oxidative stress and mitochondria, *FEBS Lett*, 497 (2001) 1-5.

[3]   Baden, D.G., and David J. Adams, Brevetoxins: Chemistry, Mechanism of Action, and

       Methods of Detection. In L.M. Botana (Ed.), *Seafood and Freshwater Toxins.*

       Pharmacology, Physiology, and Detection, Marcel Dekker, Inc., New York, Basal, 2000,

       pp. 505-532.

[4]   Baden, D.G., Bourdelais, A.J., Jacocks, H., Michelliza, S. and Naar, J., Natural and

       derivative brevetoxins: historical background, multiplicity, and effects, *Environ Health*

       Perspect, 113 (2005) 621-5.

[5]   Baden, D.G., Fuhrman, J. and Fenical, W., Oceans and Human Health: Roundtable

       Report. National Institute of Environmental Health Sciences and National Science

       Foundation, Research Triangle Park, 2001.

[6]   Belcheva, M.M. and Coscia, C.J., Diversity of G protein-coupled receptor signaling

       pathways to ERK/MAP kinase, *Neurosignals*, 11 (2002) 34-44.

[7]   Berman, F.W. and Murray, T.F., Brevetoxin-induced autocrine excitotoxicity is

       associated with manifold routes of Ca^{2+} influx, *J Neurochem*, 74 (2000) 1443-51.

[8]   Boesch, D.F., Anderson, D.M., Horner, R.A., Shumway, S.E., Tester, P.A. and

       Whitledge, T.E., Harmful Algal Blooms in Coastal Waters: Options for Prevention,

       Control and Mitigation. *An Assessment Conducted for The National Fish and Wildlife*

       Foundation and The National Oceanic and Atmospheric Administration Coastal Ocean

       Program, Center for Sponsored Coastal Ocean Research, Coastal Ocean Program,

       Chesapeake Research Consortium, Edgewater, Maryland 21037, 1997.

[9]   Bossart, G.D., Baden, D.G., Ewing, R.Y., Roberts, B. and Wright, S.D., Brevetoxicosis in

       manatees (Trichechus manatus latirostris) from the 1996 epizootic: gross, histologic, and

       immunohistochemical features, *Toxicol Pathol*, 26 (1998) 276-82.

[10]   Burgess, C., Red Flag for Fish, *Environ Health Perspect*, 109 (2001) A 178-A 179.

[11]   Catterall, W.A., Voltage-dependent gating of sodium channels: correlating structure and function., *Trends Neurosci*, 9 (1986) 7-10.

[12]   Catterall, W.A., From ionic currents to molecular mechanisms: the structure and function of voltage-gated sodium channels, *Neuron*, 26 (2000) 13-25.

[13]   Cobb, M.H. and Goldsmith, E.J., How MAP Kinases Are Regulated, *The Journal of Biological Chemistry*, 270 (1995) 14843-14846.

[14]   Davis, R.J., The mitogen-activated protein kinase signal transduction pathway, *J Biol Chem*, 268 (1993) 14553-6.

[15]   Denac, H., Mevissen, M. and Scholtysik, G., Structure, function and pharmacology of voltage-gated sodium channels, *Naunyn Schmiedebergs Arch Pharmacol*, 362 (2000) 453-79.

[16]   Ellis, S., Introduction to symposium- Brevetoxins: chemistry and pharmacology of 'red tide' toxins from *Ptychodiscus brevis* (formerly *Gymnodinium breve*), *Toxicon*, 23 (1985) 469-172.

[17]   Gawley, R.E., Rein, K.S., Jeglitsch, G., Adams, D.J., Theodorakis, E.A., Tiebes, J., Nicolaou, K.C. and Baden, D.G., The relationship of brevetoxin 'length' and A-ring functionality to binding and activity in neuronal sodium channels, *Chem Biol*, 2 (1995) 533-41.

[18]   Guy, H.R. and Seetharamulu, P., Molecular model of the action potential sodium channel, *Proc Natl Acad Sci U S A*, 83 (1986) 508-12.

[19]   Hardingham, G.E. and Bading, H., The Yin and Yang of NMDA receptor signalling, *Trends Neurosci*, 26 (2003) 81-9.

[20] Hartmann, J., Ransmayr, G. and Riederer, P., The glycine binding site of the NMDA receptor: involvement in neurodegeneration and new approach for neuroprotection, *J Neural Transm Suppl*, 43 (1994) 53-7.

[21] Hodgkin, A.L. and Huxley, A.F., A quantitative description of membrane current and its application to conduction and excitation in nerve, *J Physiol*, 117 (1952) 500-44.

[22] Hunter, T., Protein kinases and phosphatases: the yin and yang of protein phosphorylation and signaling, *Cell*, 80 (1995) 225-36.

[23] Ishida, H., Muramatsu, N., Nukaya, H., Kosuge, T. and Tsuji, K., Study on neurotoxic shellfish poisoning involving the oyster, Crassostrea gigas, in New Zealand, *Toxicon*, 34 (1996) 1050-3.

[24] Jeglitsch, G., Rein, K., Baden, D.G. and Adams, D.J., Brevetoxin-3 (PbTx-3) and its derivatives modulate single tetrodotoxin-sensitive sodium channels in rat sensory neurons, *J Pharmacol Exp Ther*, 284 (1998) 516-25.

[25] Johnson, G.L. and Lapadat, R., Mitogen-activated protein kinase pathways mediated by ERK, JNK, and p38 protein kinases, *Science*, 298 (2002) 1911-2.

[26] Mayer, M.L., Westbrook, G.L. and Guthrie, P.B., Voltage-dependent block by Mg2+ of NMDA responses in spinal cord neurones, *Nature*, 309 (1984) 261-3.

[27] Meldrum, B.S., Glutamate as a neurotransmitter in the brain: review of physiology and pathology, *J Nutr*, 130 (2000) 1007S-15S.

[28] Mori, H. and Mishina, M., Structure and function of the NMDA receptor channel, *Neuropharmacology*, 34 (1995) 1219-37.

[29]   Morris, M.D., Campbell, D.S., Taylor, T.J. and Freeman, J.I., Clinical and
       Epidemiological Features of Neurotoxic Shellfish Poisoning in North Carolina, *American
       Journal of Public Health*, 81 (1991) 471-474.

[30]   Ogata, N. and Ohishi, Y., Molecular diversity of structure and function of the voltage-
       gated Na$^+$ channels, *Jpn J Pharmacol*, 88 (2002) 365-77.

[31]   Olney, J.W., Inciting excitotoxic cytocide among central neurons, *Adv Exp Med Biol*, 203
       (1986) 631-45.

[32]   Pearson, G., Robinson, F., Beers Gibson, T., Xu, B.E., Karandikar, M., Berman, K. and
       Cobb, M.H., Mitogen-activated protein (MAP) kinase pathways: regulation and
       physiological functions, *Endocr Rev*, 22 (2001) 153-83.

[33]   Pierce, R.H., Henry, M.S., Blum, P.C., Lyons, J., Cheng, Y.S., Yazzie, D. and Zhou, Y.,
       Brevetoxin concentrations in marine aerosol: human exposure levels during a Karenia
       brevis harmful algal bloom, *Bull Environ Contam Toxicol*, 70 (2003) 161-5.

[34]   Poli, M.A., Mende, T.J. and Baden, D.G., Brevetoxins, unique activators of voltage-
       sensitive sodium channels, bind to specific sites in rat brain synaptosomes, *Mol
       Pharmacol*, 30 (1986) 129-35.

[35]   Poli, M.A., Musser, S.M., Dickey, R.W., Eilers, P.P. and Hall, S., Neurotoxic shellfish
       poisoning and brevetoxin metabolites: a case study from Florida, *Toxicon*, 38 (2000) 981-
       93.

[36]   Purkerson-Parker, S.L., Fieber, L.A., Rein, K.S., Podona, T. and Baden, D.G., Brevetoxin
       derivatives that inhibit toxin activity, *Chem Biol*, 7 (2000) 385-93.

[37]   Said, S.I., Glutamate receptors and asthmatic airway disease, *Trends Pharmacol Sci*, 20
       (1999) 132-4.

[38]   Salter, M.W., Src, N-methyl-D-aspartate (NMDA) receptors, and synaptic plasticity, *Biochem Pharmacol*, 56 (1998) 789-98.

[39]   Salter, M.W. and Kalia, L.V., Src kinases: a hub for NMDA receptor regulation, *Nat Rev Neurosci*, 5 (2004) 317-28.

[40]   Sattler, R. and Tymianski, M., Molecular mechanisms of calcium-dependent excitotoxicity, *J Mol Med*, 78 (2000) 3-13.

[41]   Stanciu, M., Wang, Y., Kentor, R., Burke, N., Watkins, S., Kress, G., Reynolds, I., Klann, E., Angiolieri, M.R., Johnson, J.W. and DeFranco, D.B., Persistent Activation of ERK Contributes to Glutamate-induced Oxidative Toxicity in a Neuronal Cell Line and Primary Cortical Neuron Cultures, *J. Biol. Chem.*, 275 (2000) 12200-12206.

[42]   Tester, P.K., P.K. Fowler, and J.T. Turner, Gulf Stream transport of the toxic red tide dinoflagellate *Ptychodiscus brevis* from Florida to North Carolina. In V.M.B. E.M. Cosper, and E.J. Carpenter (Ed.), *Coastal and Estuarine Studies, Vol. 35*, Springer Verlag, 1989, pp. 349-358.

[43]   Trainer, V.L. and Baden, D.G., High affinity binding of red tide neurotoxins to marine mammal brain, 46 (1999) 139.

[44]   Vanhoutte, P. and Bading, H., Opposing roles of synaptic and extrasynaptic NMDA receptors in neuronal calcium signalling and BDNF gene regulation, *Curr Opin Neurobiol*, 13 (2003) 366-71.

[45]   Walsh, P.J., Bookman, R.J., Zaias, J., Mayer, G.D., Abraham, W., Bourdelais, A.J. and Baden, D.G., Toxicogenomic effects of marine brevetoxins in liver and brain of mouse, *Comp Biochem Physiol B Biochem Mol Biol*, 136 (2003) 173-82.

[46]   Wang, S.Y. and Wang, G.K., Voltage-gated sodium channels as primary targets of

diverse lipid-soluble neurotoxins, *Cell Signal*, 15 (2003) 151-9.

[47]   Watkins, J.C., The Synthesis of Some Acidic Amino Acids Possessing

Neuropharmacological Activity, *J Med Pharm Chem*, 91 (1962) 1187-99.

[48]   Yu, F.H. and Catterall, W.A., Overview of the voltage-gated sodium channel family,

Genome Biol, 4 (2003) 207.

CHAPTER 2

CHARACTERIZATION OF BREVETOXIN- AND POTASSIUM-INDUCED

DEPOLARIZATION IN NEOCORTICAL NEURONS USING MEMBRANE POTENTIAL-

SENSITIVE FLUORESCENT DYES.

_____

ABSTRACT

      Brevetoxins (PbTx1-10) represent a series of structurally related polyether neurotoxins

that are produced by the dinoflagellate *Karenia brevis* and have been implicated in numerous

epizootics in the Gulf of Mexico. Brevetoxins pose a threat to humans inasmuch as consumption

of shellfish contaminated with the toxin is associated with Neurotoxic Shellfish Poisoning, a

syndrome involving both gastroenteritis and neurological sequelae. Brevetoxin exerts its effects

by binding to voltage-gated sodium channels (VGSC) in the brain and altering their gating

properties resulting in the propagation of continuous action potentials in neurons. Due to

brevetoxin's ability to depolarize neurons, this depolarization may lend itself to measurement

using membrane potential-sensitive fluorescent dyes. We have accordingly optimized assay

conditions for two such dyes using murine neocortical cells in primary culture. We compared

two dyes, DiBAC$_4$(3) and the Membrane Potential Assay Kit (FMPblue, Molecular Devices Inc.,

blue dye) in an effort to optimize these assays for intact neurons. We found that with DiBAC$_4$(3)

a dye concentration of 2.5 μM provided the optimum signal, whereas FMPblue gave the greatest

signal at one-half the manufacturer suggested concentration. Using these techniques, we further

developed standard conditions that allowed us to quantify the magnitude of PbTx-2-induced

depolarization through comparison to that produced by KCl in neocortical cells. This analysis

allowed us to determine that 300 nM PbTx-2 and 15 mM KCl both depolarized neocortical

neurons to a membrane potential (E_M) of –60 mV. The use of concentrations of brevetoxin and

KCl that produce equivalent levels of depolarization will further permit mechanistic studies

exploring brevetoxin's influence on neuronal signaling.

INTRODUCTION

Brevetoxins (PbTx1-10) represent a series of structurally related polyether, lipophilic neurotoxins produced by the dinoflagellate *Karenia brevis* (formerly, *Ptychodiscus brevis* and *Gymnodinium breve*) [24]. These neurotoxins have been linked to periodic 'red tide' blooms, which are known to occur in the Gulf of Mexico as well as off the coasts of New Zealand and Japan [4,13,18,27]. Ingestion of contaminated shellfish can give rise to a syndrome known as Neurotoxic Shellfish Poisoning (NSP) characterized by symptoms including nausea, cramps, diarrhea, and various neurological sequelae [22]. Exposure to brevetoxin also occurs through inhalation of marine aerosols during red tide events. Inhalation exposure is known to cause respiratory irritation and asthma-like symptoms such as cough, watery eyes, and bronchoconstriction as well as dizziness, tunnel vision and skin rashes [14].

Brevetoxins bind to neurotoxin site 5 of voltage gated sodium channels (VGSCs) in neural tissue. This binding results in an augmentation of VGSC function causing a shift in the activation potential to more negative values, prolongation of mean channel open time and inhibition of channel inactivation. These effects may induce a state of repetitive action potentials. Brevetoxin-induced depolarization of cerebellar granule neurons in culture results in excessive glutamate release and overactivation of *N*-methyl-D-aspartate receptors (NMDAR) [3,6,19]. Due to their Ca^{2+} permeability, exaggerated activation of NMDARs leads to a massive influx of extracellular Ca^{2+} that initiates a cascade of events eventually leading to cell death [2,7]. These effects contribute to the phenomenon known as excitotoxicity. As first coined by Olney, an excitotoxic event is defined by the initiation of excessive excitatory amino acid release and subsequent overactivation of glutamate receptors [1,23,25]. The resulting Ca^{2+} overload ultimately leads to neuronal degeneration [1,23,25].

In previous studies, brevetoxin's ability to augment NMDAR-stimulated Ca^{2+} influx with subsequent activation of extracellular signal-regulated protein kinase (ERK1/2) was demonstrated [10,11]. ERK1/2 represents a subfamily of the mitogen-activated protein kinases believed to participate in NMDAR-induced changes in synaptic plasticity, learning and memory, as well as in neuronal growth and survival [10,26]. PbTx-2-induced ERK1/2 activation was Ca^{2+} dependent and mediated by Ca^{2+} entry through manifold routes [10]. Further characterization of the role of NMDARs in PbTx-modulation of cerebral cortical neurons was examined through fluorescence monitoring of spontaneous Ca^{2+} oscillations. These data indicated that functional upregulation of NMDARs was produced by PbTx, and was attributed to two primary mechanisms: Src kinase-induced tyrosine phosphorylation of NMDARs and removal of the voltage-dependent Mg^{2+} block [11]. In order to further distinguish between these possible mechanisms, we utilized membrane-potential sensitive fluorometric dyes to quantify brevetoxin and KCl-induced membrane depolarization in neocortical cell populations.

Membrane-potential sensitive dyes are lipophilic, anionic compounds whose distribution across the cell membrane is dependent upon the membrane potential of the cell. After addition to cells in culture, these dyes partition across the cell membrane coming to equilibrium prior to the introduction of a drug or stimulus that depolarizes cells. The membrane potential dependent movement of anionic dye molecules across the cell membrane follows a Nernst equation and dye binding to cellular proteins produces an increase in the fluorescence quantum yield and peak shift in both excitation and emission wavelengths [8,5,30]. In the present study, this increment in fluorescent signal was measured using a Fluorometric Imaging Plate Reader (FLIPR® Molecular Devices, Inc.). This method of fluorescence assessment of membrane potential was determined using two different membrane potential-sensitive fluorescent dyes, $DiBAC_4(3)$

(DiBAC) and the FLIPR Membrane Potential Assay Kit blue dye (FMPblue). A method to directly assess the membrane potential of populations of neurons in culture was developed, and a KCl reference standard was used to quantify PbTx-2-induced changes in membrane potential. This ability to quantify the amount of membrane depolarization using a membrane potential-sensitive fluorescent dye further permitted a mechanism by which brevetoxin's depolarizing influence on excitatory signaling in neurons could be explored.

MATERIALS AND METHODS

Neocortical Neuron Culture: Primary cell cultures of neocortical neurons were obtained from Swiss-Webster mice on embryonic day 16. Embryos were extracted following euthanasia via CO_2 asphyxiation and their neocortices were collected. Isolated neocortices were then removed of their meninges, minced by trituration using a Pasteur pipette, and treated with trypsin for 25 minutes at 37ºC. The cells were further dissociated via two successive trituration and sedimentation steps in isolation buffer containing soybean trypsin inhibitor and DNase. The cells underwent another centrifugation step and were resuspended in a neuron-plating medium containing Eagle's minimal essential medium with Earle's salt (MEM), along with 2 mM L-glutamine, 10% fetal bovine serum, 10% horse serum, 100 I.U./ml penicillin and 0.10 mg/ml streptomycin, pH=7.4. Cells were plated onto poly-L-lysine treated, 96 (9 mm) well, black, clear-bottomed culture plates at a density of 1 X 10^6 cells/well. Plates were incubated at 37ºC with 5% CO_2 and 95% humidity. On day 2, post-plating, cells were treated with cytosine arabinoside (10 μM) to prevent proliferation of non-neuronal cells. The culture media was changed both on days 5, 8, and 11 using a serum-free growth medium containing 1X Neurobasal Medium supplemented with B-27 (Invitrogen), 100 I.U./ml penicillin, 0.10 mg/ml streptomycin,

23

and 0.2 mM L-glutamine. Cultures were used in experiments between 8-11 days *in vitro*. All animal use protocols were approved by the Institutional Animal Care and Use Committee (IACUC).

DiBAC$_4$(3) Fluorescence Monitoring: In order to monitor fluorescence using DiBAC$_4$(3), all growth media was aspirated and cells were washed four times with Locke's buffer (154 mM NaCl, 5.6 mM KCl, 1.0 mM MgCl2, 2.3 mM CaCl2, 8.6 mM HEPES, 5.6 mM glucose, and 0.1 mM glycine, pH=7.4) leaving 100 µl in each well. 100 µl DiBAC$_4$(3) was then added at 2X the final desired concentration and the plates were allowed to incubate at room temperature for 1 hr. All drug solutions were made at 10X the final desired concentration and 20 µl was added to each well. Fluorescence was measured using a Fluorometric Imaging Plate Reader (FLIPR, Molecular Devices, Sunnyvale, CA) where neurons were excited to 488 nm and DiBAC$_4$(3) emission was measured within 510 nm-570 nm. Fluorescence was recorded using a CCD camera with a shutter speed of 0.6 sec and a laser power of 0.1 W to ensure an average baseline fluorescence of 20,000 to 30,000 arbitrary units. The baseline fluorescence was recorded prior to each experiment to ensure normality across the plate.

Membrane Potential Assay Kit Fluorescence Monitoring: Cells were removed of their media and 100 µl of Locke's buffer was added to each well. Dye concentrations were made up at 2X the desired concentration and 100 µl was added to the set wells. Cells were then incubated at room temperature for 30 mins. Again, all drug solutions were made up at 10X the final desired concentration and 20 µl was added to each well. Fluorescence was measured using FLIPR (Molecular Devices, Sunnyvale, CA) and a #2 filter (540-590 nM bandpass). Neurons were excited to 530 nm and emission was measured within 550-565 nm. Exposure length (~0.7 sec) and laser power (~0.1 W) were adjusted to provide an average fluorescence of 7,000-10,000

units. Prior to each experiment, a baseline fluorescence was recorded to verify that the dye had come to equilibrium.

Materials: Trypsin, penicillin, streptomycin, heat-inactivated fetal bovine serum, horse serum and soybean trypsin inhibitor were obtained from Atlanta Biologicals (Norcross, GA). Minimum essential medium (MEM), Deoxyribonuclease (DNase), poly-L-lysine, and cytosine arabinoside were purchased from Sigma (St. Louis, MO). Neurobasal and B-27 Supplement were purchased from Invitrogen Corporation (Carlsbad, CA). Tetrodotoxin (TTX) and brevetoxin-2 (PbTx-2) were purchased from Tocris Cookson, Inc. (Ellisville, MO). DiBAC and FLIPR® Membrane Potential Assay Kit were purchased from Molecular Devices (Sunnyvale, CA).). Anti-p44/42 and anti- phospho-p44/42 antibodies were purchased from Cell Signaling Technology (Beverly, MA).

Data Analysis: Data analysis and curve fitting were completed using GraphPad Prism® (GraphPad Software, Inc., San Diego, CA). All fluorescence monitoring was subject to spatial uniformity correction to ensure normality across the plate. The spatial uniformity correction was calculated by FLIPR as follows: normalized fluorescence value = (average of all initial fluorescence values)/(initial fluorescence of each well) X (fluorescence value of each well).

RESULTS

Optimal fluorescence in neocortical cells is achieved with 2.5 μM DiBAC$_4$(3)

Neocortical neurons exhibit changes in fluorescence in response to a depolarization stimulus due to the accumulation of negatively charged dye and subsequent increase in fluorescence quantum efficiency. DiBAC$_4$(3), a lipophilic, anionic dye, was utilized at three different concentrations to determine the optimal dye concentration for use in neocortical cells in

culture. When monitoring fluorescence using 5 μM DiBAC, the change in fluorescence from

basal to maximum upon the addition of 33 mM KCl was approximately 3600 relative fluorescent

units (rfu) (Fig. 2.1A). This maximum fluorescent signal was increased two-fold using 2.5 μM

$DiBAC_4(3)$, which produced a maximum change in fluorescence of 6000 rfu in response to 33

mM KCl (Fig. 2.1B). A final concentration of 1 μM $DiBAC_4(3)$ generated the smallest signal as

reflected in the response to 33 mM KCl which produced a maximum change in fluorescence of

only 2000 rfu; the corresponding linear regression using the maximum values at each KCl

concentration yielded an extremely shallow slope (Fig. 2.1C, D). These data indicate that the

optimum dye concentration of $DiBAC_4(3)$ was 2.5 μM inasmuch as this concentration produced

the greatest fluorescent signal in neocortical neurons in culture. Using all three $DiBAC_4(3)$

concentrations, KCl produced a concentration dependent increase in maximum fluorescence

consistent with a depolarization-induced redistribution of the lipophilic anion dye with attendant

increase in fluorescence quantum efficiency.

$DiBAC_4(3)$ as an indicator of membrane depolarization

Using 2.5 μM $DiBAC_4(3)$, a KCl concentration-response curve was generated to establish

that fluorescent intensity was directly proportional to the extracellular K^+ concentration. Linear

regression analysis of the maximum change in fluorescence at each concentration of KCl was

therefore performed (Fig 2.2A, B). For a Nernstian fluorescent indicator of membrane potential,

the ratio of fluorescence inside to the outside of the cell should be related to the membrane

potential as described by the Nernst equation [12]. This prediction is based on the principal that

the membrane potential of isolated neurons is largely the result of the K^+ diffusion potential [11].

We therefore used a modified Goldman equation,

$$E_m = \frac{RT}{F} \ln \frac{P_K[K^+]_{out} + P_{Na}[Na^+]_{out}}{P_K[K^+]_{in} + P_{Na}[Na^+]_{in}}$$

to generate a standard curve for the estimation of membrane potential (E_M) at various

concentrations of extracellular K^+ (Fig. 2.2C). These estimates of neuronal E_M were then plotted

against the log concentration of KCl (Fig. 2.2C). The membrane potential of neocortical neurons

was dependent on the external concentration of K^+, and the slope of the $\log[K^+]_o$ versus E_M was

59.5 ± 0.45 which is that anticipated for E_M determined exclusively by the K^+ gradient [16]. The

concordance of the $[K^+]_o$ versus membrane fluorescence and $[K^+]_o$ versus E_M regressions indicate

that changes in neocortical cell $DiBAC_4(3)$ fluorescence can be used to estimate membrane

potential. Therefore, the fluorescence changes for each concentration of KCl were regressed to

the calculated E_M values to produce a standard curve for measurement of brevetoxin-induced

changes in the membrane potential of neocortical cells (Fig. 2.2D).

Estimation of PbTx-2-induced changes in membrane potential

Inasmuch as brevetoxin has been shown to depolarize neurons, this depolarization was

assessed in the same manner as KCl with neocortical neurons in culture. Neurons were treated

with different concentrations of PbTx-2 and fluorescence response was monitored in $DiBAC_4(3)$

loaded neurons (Fig. 2.3A). The highest concentration of PbTx-2, 1 μM, exhibited a change in

$DiBAC_4(3)$ fluorescent signal of approximately 5000 rfu relative to control fluorescence (Fig.

2.3A). A concentration-response curve of the maximum change in fluorescence values for each

concentration of PbTx-2 was fitted using a three parameter logistic equation that yielded an EC_{50}

of 69.2 nM with a 95% CI of 5.8 to 830 nM (Fig. 2.3B). This concentration-response curve also

provided a means by which the membrane potential produced by PbTx-2-induced depolarization

could be quantified through comparison to the reference data obtained with increments in $[K^+]_o$ (Fig. 2.2D). The relationship between maximum change in $DiBAC_4(3)$ fluorescence and E_M (Fig. 2D) was accordingly used to assign a membrane potential value to the increments in fluorescence produced by each concentration of PbTx-2 (Fig. 2.3C). A concentration-response curve for PbTx-2-induced depolarization was then generated; this yielded a PbTx-2 EC_{50} of 70 nM with a 95% CI of 68 to 73 nM (Fig. 2.3D). These data moreover allowed the subsequent determination of concentrations of $[K^+]_o$ and PbTx-2 that produce equivalent levels of depolarization in neocortical neurons (Table 2.1).

PbTx-2-induced depolarization is a consequence of voltage-gated sodium channel activation

Brevetoxin exerts its neurotoxic effects through the binding to voltage-gated sodium channel (VGSC) alpha subunits. This role of VGSCs in PbTx-2-induced depolarization was established by treating cells with 1 μM tetrodotoxin (TTX), a VGSC antagonist, and measuring PbTx-2-induced changes in relative fluorescence. Although 1 μM TTX did not affect the depolarization response to an increase in extracellular $[K^+]$ (Fig. 2.4A, B), the PbTx-2-induced fluorescent increments were essentially eliminated (Fig. 2.4C, D). This antagonism demonstrates the involvement of VGSCs in PbTx-2-induced depolarization.

Comparison of the Membrane Potential Assay Kit, blue dye

The FLIPR Membrane Potential Assay Kit (FMPblue), blue dye, is a lipophilic, anionic, bis-oxonol based dye that distributes across the cell membrane as a function of membrane potential, and displays enhanced fluorescence emission following binding to intracellular proteins. This kit also contains a proprietary extracellular fluorescence quencher that eliminates

the need to wash neurons before and after the dye loading incubation. After monitoring the

fluorescence of neocortical neurons in cultures exposed to differing concentrations of FMPblue,

an optimum dye concentration was determined to be one-half the suggested manufacturer

concentration (1/2X). This concentration provided a maximum increment in fluorescence of

over 7000 rfu and the greatest signal to noise ratios in response to an elevation of extracellular

KCl (Fig. 2.5B). The manufacturer-suggested concentration (1X) gave a maximum fluorescence

increase of 6801 rfu with a signal to noise ratio slightly lower than that of 1/2X (Fig. 2.5A). A

dye concentration of one-fourth the manufacturer suggested concentration (1/4X) provided a

KCl-induced fluorescence increment of 5021 rfu (Fig. 2.5C). Lastly, a dye concentration of one-

eighth the suggested concentration resulted in a maximum signal of only 2309 rfu in response to

KCl and was therefore insufficient to measure membrane potential in neocortical neurons (Fig.

2.5D). A summary of these data is depicted in Figure 2.5e.

FMPblue as an indicator of membrane depolarization

Using an FMPblue dye concentration of 1/2X, cells were treated with increasing

concentrations of KCl and fluorescence was measured (Fig. 2.6A). The resulting linear

regression for KCl-induced increase in fluorescence (Fig. 2.6B) was superimposable with the

standard curve for $[K^+]_e$ -induced change in membrane potential (Fig. 2.6C). These data again

indicate that, similar to $DiBAC_4(3)$, FMPblue behaved as a Nernstian dye and fluorescence

values for each concentration of KCl were plotted against the calculated E_M values to provide a

means of equating changes in fluorescence intensity with alterations in membrane potential (Fig.

2.6D).

Comparison of PbTx-2 and KCl in FMPblue-loaded neocortical neurons

PbTx-2 treatment of neocortical neurons produced a depolarization with concomitant increments in fluorescent emission similar to that produced by an increase in $[K^+]_o$. As with $DiBAC_4(3)$, increasing concentrations of PbTx-2 were added to neuronal cultures and fluorescence output using FMPblue was monitored (Fig. 2.7A). A concentration of 1 μM PbTx-2 produced the greatest fluorescence signal with a maximum change in fluorescence of 1867 rfu. A PbTx-2 concentration-response curve was generated plotting the log of each PbTx-2 concentration against its corresponding maximum change in fluorescence (Fig. 2.7B). Nonlinear regression analysis of the PbTx-2-induced changes in maximum FMPblue fluorescence yielded an EC_{50} value of 60.9 nM with a 95% CI of 46.9 to 79 nM. Using the KCl-induced changes in fluorescence and E_M values as a reference (Fig. 2.6D), changes in cellular fluorescence for each concentration of PbTx-2 (Fig. 2.7C) were then used to determine the corresponding E_M value and plotted as a function of PbTx-2 concentration (Fig. 2.7D). Nonlinear regression analysis yielded an EC_{50} value of 61.1 nM with a 95% CI of 49.4 to 75.4 nM for PbTx-2-induced changes in E_M in FMPblue loaded neurons. We found that 300 nM PbTx-2 produced a depolarization of neurons to a membrane potential of approximately –60 mV. Our results with KCl indicate that this level of depolarization is equivalent to that produced by 15 mM KCl (Table 2.2).

PbTx-2-induced depolarization occurs via voltage-gated sodium channels.

TTX did not affect the KCl-induced increase in FMPblue fluorescence (Fig. 2.8A, B), whereas it effectively eliminated the response induced by PbTx-2 (Fig. 2.8C, D). These data again demonstrate the involvement of VGSCs in PbTx-2-induced depolarization.

Equivalent levels of membrane depolarization are induced by 300nM PbTx-2 and 15mM KCl

To verify our calculations, we used FMPblue to monitor changes in fluorescence induced by 15 mM KCl and 300 nM PbTx-2. We found that both 15 mM KCl and 300 nM PbTx-2 produced a maximum change in fluorescence yield of approximately 1500 rfu (Fig. 2.9). This data, along with our findings suggesting the inference of membrane potential from fluorescence quantum yield, supports our conclusion that these concentrations of KCl and PbTx-2 induce equivalent levels of depolarization.

Extracellular signal-regulated protein kinase (ERK1/2) phosphorylation is dependent on Na^+ influx through voltage-gated sodium channels (VGSC).

In neocortical neurons, TTX has been found to decrease PbTx-induced ERK1/2 phosphorylation *in vitro*, an effect found to be mediated by Ca^{2+} influx through NMDA receptors [10]. Using concentrations of KCl and PbTx-2 that produce equivalent changes in membrane potential, the effects of depolarization versus sodium influx on this NMDAR-mediated ERK1/2 activation could be compared. We found that ERK1/2 phosphorylation was increased significantly by both 15 mM KCl and 300 nM PbTx-2 (Fig. 2.10A). The levels of KCl- and PbTx-induced ERK1/2 activation differed only slightly as they were increased respectively to 2.38 ± 0.62 and 2.26 ± 0.34 percent of control (Fig. 2.10B). KCl-induced ERK1/2 phosphorylation was inhibited, however, after the addition of TTX (1 μM) resulting in 1.14 ± 0.19 percent of control (Fig. 2.10B). This data, in junction with our previous findings where TTX inhibited PbTx-2-induced depolarization yet failed to inhibit that induced by KCl, suggests the dependence of ERK1/2 activation on Na^+ influx through VGSCs.

DISCUSSION

The standard for monitoring changes in membrane potential is patch-clamp recording [15]. However, this technique, due to its low throughput and cost of instrumentation, is inappropriate for the development of high-throughput screening (HTS) assays to measure membrane potential changes at the population level [31]. Measurement of membrane potential in populations of cells moreover avoids any bias associated with choosing cells that are easily impaled. Previous studies in non-neuronal cells have been performed using the membrane potential-sensitive dyes $DiBAC_4(3)$ and FMPblue, and have found a strong correlation between these responses and those of traditional patch-clamp techniques [5]. These fluorescent dyes provide a fast, high throughput, method for observing changes in membrane potential and therefore provide a practical means of monitoring ion channel behavior in cells. In previous studies, fluorescent dyes have been used in various transformed cell lines but have yet to be optimized in primary cultures of neocortical neurons [5,9,20,21,28,31]. We have compared $DiBAC_4(3)$ and FMPblue in neocortical neurons to optimize assay conditions for these cells and to develop a method for measuring PbTx-2-induced depolarization. This method will afford further characterization of PbTx-2 actions on intact neurons and exploration of mechanisms underlying its excitotoxic effects.

In the current study, we found that $DiBAC_4(3)$ provides an optimum fluorescence signal in neocortical cells when used at 2.5 μM. The lower signal at 5 μM $DiBAC_4(3)$ may be attributed to the cytotoxic effects of a concentration too high for neocortical cells. FMPblue gave similar results inasmuch as it provides an optimum signal at one-half the manufacturer-suggested concentration, and can be utilized at concentrations as low as one-fourth that concentration with adequate fluorescence output. FMPblue provided an improvement in the

32

fluorescence assay in that it was characterized by an increase in the signal to noise ratio. An added benefit of this dye was it's more rapid response times as compared to $DiBAC_4(3)$. These data with neurons correlate well with previous studies in which the two dyes were compared and indicate the use of membrane-potential sensitive fluorescent dyes as a practical and efficient method in detecting changes in membrane potential in primary cultures of neocortical neurons [5,15,30,31].

Brevetoxin has been shown to increase intracellular Na^+ concentrations through binding to neurotoxin site 5 on VGSCs [29]. Tetrodotoxin (TTX), an antagonist of VGSCs, inhibits both PbTx -induced Na^+ current in rat sensory neurons and the subsequent ERK1/2 activation in neocortical neurons [10,19]. In the results reported herein, TTX had no effect on the fluorescent signal produced by an elevation of extracellular K^+ whereas it inhibited the increment in fluorescent signal produced by brevetoxin in neocortical cells. These data agree with previous reports in which TTX prevented PbTx-induced depolarization while having no effect on potassium channels [17]. These findings support the notion that brevetoxin exerts its depolarizing influence through an alteration of VGSC gating properties.

To better quantify PbTx-2 modulation of neuronal excitability, we utilized extracellular K^+ as a reference for linking changes in fluorescence with membrane potential (E_M). This permitted quantification of PbTx-induced changes in neuronal E_M. Using this approach we found that 15 mM KCl and 300 nM PbTx-2 produced equivalent maximum changes in fluorescent emission and therefore represent concentrations that produce an equivalent E_M of approximately –60 mV. Using concentrations of PbTx and KCl that produce equivalent levels of depolarization, experiments with TTX were implemented to distinguish between depolarization per se versus Na^+ influx as essential for PbTx augmentation of NMDAR function.

In previous studies, Na^+ has been suggested not only to participate in the depolarization-mediated removal of the NMDAR Mg^{2+} blockade but to also more specifically play a role in NMDAR upregulation through interaction with the receptor. These studies have found that an increase in intracellular Na^+ causes an upregulation of NMDAR function [32,33]. PbTx-2 has been shown to augment NMDAR-mediated ERK2 activation and that this augmentation is not only dependent on Na^+ influx through VGSCs but also on the augmentation of Ca^{2+} influx through the NMDAR [10,11]. To further assess the role of Na^+ in the upregulation of the NMDAR, we examined the effect of TTX on K^+-induced ERK1/2 activation using 15 mM KCl, a concentration demonstrated to produce an equivalent level of depolarization as that induced by 300 nM PbTx-2. Previously, PbTx-2-induced ERK1/2 activation has been shown to be inhibited by TTX and thus mediated by VGSC activation [10]. In the current study, ERK1/2 activation induced by 15 mM KCl was inhibited by TTX as well. This data, in junction with our previous findings where KCl-induced depolarization was found to occur independent of Na^+ influx, demonstrates a separation between the effects of $[Na^+]_i$ and depolarization. These data suggest that depolarization and subsequent removal of the voltage-dependent Mg^{2+} block do not result in ERK1/2 activation alone, but rather it is the increment in $[Na^+]_i$ that is required for ERK1/2 activation. Therefore, the ability of Na^+ to augment NMDARs appears to be involved in PbTx-2-induced ERK1/2 activation.

Revealing the mechanisms underlying brevetoxin-induced neurotoxicity is not only important in the development of interventions for toxin exposure but also to provide insight in a variety of pathological disorders involving channelopathies that manifest as conditions such as paralysis, epilepsy, and ataxia.

REFERENCES

[1]   Arundine, M. and Tymianski, M., Molecular mechanisms of calcium-dependent

         neurodegeneration in excitotoxicity, *Cell Calcium*, 34 (2003) 325-37.

[2]   Atlante, A., Calissano, P., Bobba, A., Giannattasio, S., Marra, E. and Passarella, S.,

         Glutamate neurotoxicity, oxidative stress and mitochondria, *FEBS Lett*, 497 (2001) 1-5.

[3]   Baden, D.G., Brevetoxins: unique polyether dinoflagellate toxins, *Faseb J*, 3 (1989)

         1807-17.

[4]   Baden, D.G., and David J. Adams, Brevetoxins: Chemistry, Mechanism of Action, and

         Methods of Detection. In L.M. Botana (Ed.), *Seafood and Freshwater Toxins.*

         Pharmacology, Physiology, and Detection, Marcel Dekker, Inc., New York, Basal, 2000,

         pp. 505-532.

[5]   Baxter, D.F., Kirk, M., Garcia, A.F., Raimondi, A., Holmqvist, M.H., Flint, K.K.,

         Bojanic, D., Distefano, P.S., Curtis, R. and Xie, Y., A novel membrane potential-

         sensitive fluorescent dye improves cell-based assays for ion channels, *J Biomol Screen*, 7

         (2002) 79-85.

[6]   Berman, F.W. and Murray, T.F., Brevetoxins cause acute excitotoxicity in primary

         cultures of rat cerebellar granule neurons, *J Pharmacol Exp Ther*, 290 (1999) 439-44.

[7]   Berman, F.W. and Murray, T.F., Brevetoxin-induced autocrine excitotoxicity is

         associated with manifold routes of Ca^{2+} influx, *J Neurochem*, 74 (2000) 1443-51.

[8]   Brauner, T., Hulser, D.F. and Strasser, R.J., Comparative measurements of membrane

         potentials with microelectrodes and voltage-sensitive dyes, *Biochim Biophys Acta*, 771

         (1984) 208-16.

[9]   Dall'Asta, V., Gatti, R., Orlandini, G., Rossi, P.A., Rotoli, B.M., Sala, R., Bussolati, O. and Gazzola, G.C., Membrane potential changes visualized in complete growth media through confocal laser scanning microscopy of bis-oxonol-loaded cells, *Exp Cell Res*, 231 (1997) 260-8.

[10]   Dravid, S.M., Baden, D.G. and Murray, T.F., Brevetoxin activation of voltage-gated sodium channels regulates Ca dynamics and ERK1/2 phosphorylation in murine neocortical neurons, *J Neurochem*, 89 (2004) 739-49.

[11]   Dravid, S.M., Baden, D.G. and Murray, T.F., Brevetoxin augments NMDA receptor signaling in murine neocortical neurons, *Brain Res*, 1031 (2005) 30-8.

[12]   Ehrenberg, B., Montana, V., Wei, M.D., Wuskell, J.P. and Loew, L.M., Membrane potential can be determined in individual cells from the nernstian distribution of cationic dyes, *Biophys J*, 53 (1988) 785-94.

[13]   Ellis, S., Introduction to symposium- Brevetoxins: chemistry and pharmacology of 'red tide' toxins from *Ptychodiscus brevis* (formerly *Gymnodinium breve*), *Toxicon*, 23 (1985) 469-172.

[14]   Fleming, L.E. and Baden, D.G., Florida Red Tide and Human Health: Background. NIEHS Marine and Freshwater Biomedical Sciences Center, University of Miami School of Medicine, Miami, FL, 1999.

[15]   Gonzalez, J.E., Oades, K., Leychkis, Y., Harootunian, A. and Negulescu, P.A., Cell-based assays and instrumentation for screening ion-channel targets, *Drug Discovery Today*, 4 (1999) 431-439.

[16]   Hille, B., Ionic Channels of Excitable Membranes. Sinauer Associates, Inc., Sunderland, MA., 1992, pp. 403-411.

[17] Huang, J.M., Wu, C.H. and Baden, D.G., Depolarizing action of a red-tide dinoflagellate brevetoxin on axonal membranes, *J Pharmacol Exp Ther*, 229 (1984) 615-21.

[18] Ishida, H., Muramatsu, N., Nukaya, H., Kosuge, T. and Tsuji, K., Study on neurotoxic shellfish poisoning involving the oyster, Crassostrea gigas, in New Zealand, *Toxicon*, 34 (1996) 1050-3.

[19] Jeglitsch, G., Rein, K., Baden, D.G. and Adams, D.J., Brevetoxin-3 (PbTx-3) and its derivatives modulate single tetrodotoxin-sensitive sodium channels in rat sensory neurons, *J Pharmacol Exp Ther*, 284 (1998) 516-25.

[20] Jensen, A.A. and Kristiansen, U., Functional characterisation of the human alpha1 glycine receptor in a fluorescence-based membrane potential assay, *Biochem Pharmacol*, 67 (2004) 1789-99.

[21] Lichtshtein, D., Kaback, H.R. and Blume, A.J., Use of a lipophilic cation for determination of membrane potential in neuroblastoma-glioma hybrid cell suspensions., *Proc. Natl. Acad. Sci. USA*, 76 (1979) 650-654.

[22] Morris, M.D., Campbell, D.S., Taylor, T.J. and Freeman, J.I., Clinical and Epidemiological Features of Neurotoxic Shellfish Poisoning in North Carolina, *American Journal of Public Health*, 81 (1991) 471-474.

[23] Olney, J.W., Brain lesions, obesity, and other disturbances in mice treated with monosodium glutamate, *Science*, 164 (1969) 719-21.

[24] Purkerson-Parker, S.L., Fieber, L.A., Rein, K.S., Podona, T. and Baden, D.G., Brevetoxin derivatives that inhibit toxin activity, *Chem Biol*, 7 (2000) 385-93.

[25] Rothman, S.M. and Olney, J.W., Excitotoxicity and the NMDA receptor--still lethal after eight years, *Trends Neurosci*, 18 (1995) 57-8.

[26]   Sweatt, J.D., The neuronal MAP kinase cascade: a biochemical signal integration system subserving synaptic plasticity and memory, *J Neurochem*, 76 (2001) 1-10.

[27]   Tester, P.K., P.K. Fowler, and J.T. Turner, Gulf Stream transport of the toxic red tide dinoflagellate *Ptychodiscus brevis* from Florida to North Carolina. In V.M.B. E.M. Cosper, and E.J. Carpenter (Ed.), *Coastal and Estuarine Studies, Vol. 35*, Springer Verlag, 1989, pp. 349-358.

[28]   Vickery, R.G., Amagasu, S.M., Chang, R., Mai, N., Kaufman, E., Martin, J., Hembrador, J., O'Keefe, M.D., Gee, C., Marquess, D. and Smith, J.A., Comparison of the pharmacological properties of rat Na(V)1.8 with rat Na(V)1.2a and human Na(V)1.5 voltage-gated sodium channel subtypes using a membrane potential sensitive dye and FLIPR, *Receptors Channels*, 10 (2004) 11-23.

[29]   Wang, S.Y. and Wang, G.K., Voltage-gated sodium channels as primary targets of diverse lipid-soluble neurotoxins, *Cell Signal*, 15 (2003) 151-9.

[30]   Whiteaker, K.L., Gopalakrishnan, S.M., Groebe, D., Shieh, C.C., Warrior, U., Burns, D.J., Coghlan, M.J., Scott, V.E. and Gopalakrishnan, M., Validation of FLIPR membrane potential dye for high throughput screening of potassium channel modulators, *J Biomol Screen*, 6 (2001) 305-12.

[31]   Wolff, C., Fuks, B. and Chatelain, P., Comparative study of membrane potential-sensitive fluorescent probes and their use in ion channel screening assays, *J Biomol Screen*, 8 (2003) 533-43.

[32]   Xin, W.K., Kwan, C.L., Zhao, X.H., Xu, J., Ellen, R.P., McCulloch, C.A. and Yu, X.M., A functional interaction of sodium and calcium in the regulation of NMDA receptor activity by remote NMDA receptors, *J Neurosci*, 25 (2005) 139-48.

[33]   Yu, X.M. and Salter, M.W., Gain control of NMDA-receptor currents by intracellular sodium, *Nature*, 396 (1998) 469-74.

A.

5μM DiBAC

□ 33mM KCl
● 23mM KCl
▼ 13mM KCl
▼ 8mM KCl
▲ 3mM KCl

B.

2.5μM DiBAC

□ 33mM KCl
● 23mM KCl
■ 18mM KCl
♦ 13mM KCl
▼ 8mM KCl
▲ 3mM KCl

C.

1μM DiBAC

□ 33mM KCl
● 23mM KCl
♦ 13mM KCl
▼ 8mM KCl
▲ 3mM KCl

D.

[DiBAC] Comparison

—— 5uM DiBAC
– – 2.5uM DiBAC
---- 1uM DiBAC
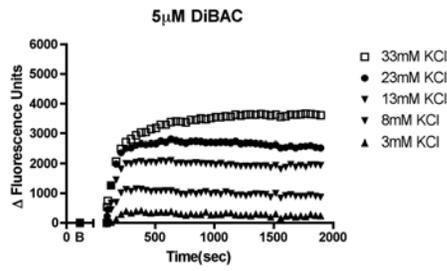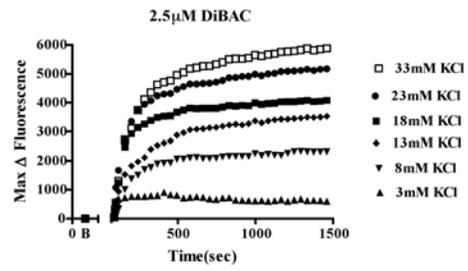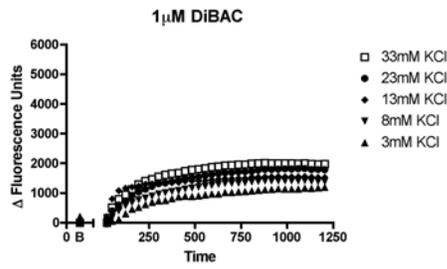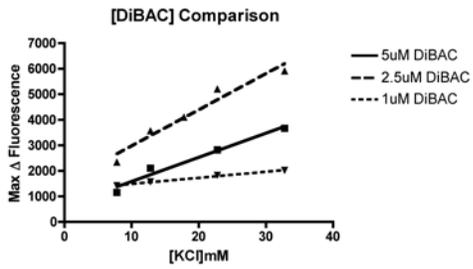
Figure 2.1. *Change in fluorescence intensity as a function of DiBAC$_4$(3) concentration in neocortical cells.* Data depicted are from a representative experiment that was repeated three times. In D, each point represents the maximum change in fluorescence induced at each indicated KCl concentration.

40

A.

B.

C.

D.
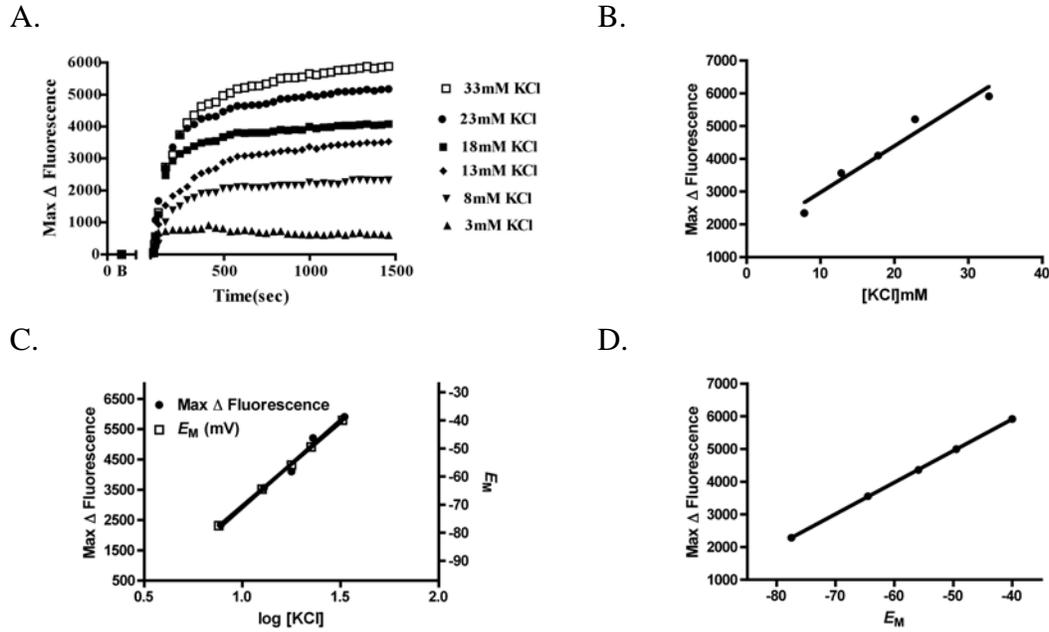
Figure 2.2. *KCl-induced changes in membrane potential can be measured using the membrane-potential sensitive fluorescent dye, DiBAC$_4$(3).* In A, fluorescence output was monitored over time as a function of [KCl] and then plotted as maximum change in fluorescence. In B, each point represents the maximum change in fluorescence units induced by each concentration of KCl. In C, a comparison of the regressions for log[KCl] induced increments in fluorescence and calculated EM values derived from the Goldman equation. In D, the maximum change in fluorescence is plotted against the membrane potential induced by each concentration of KCl.

A.

B.

C.

D.
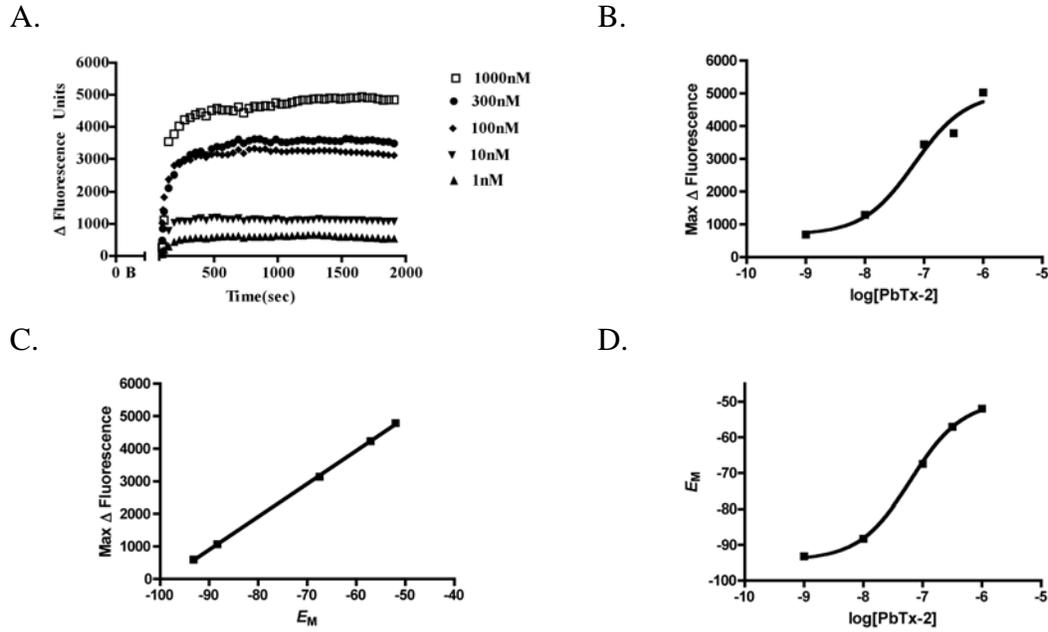
Figure 2.3. *PbTx-2-induced changes in membrane potential can be measured by comparison of fluorescence output with that achieved by an increase in extracellular K^+ using $DiBAC_4(3)$.* In A, fluorescence output was monitored over time as a function of [KCl] and then plotted as maximum change in fluorescence. In B, non-linear regression analysis of the maximum change in fluorescence for each concentration of PbTx-2 was performed. In C, increments in fluorescent responses for each concentration of PbTx-2 were regressed to the corresponding values from KCl-induced changes in membrane potential reference plot. In D, each point represents the membrane potential induced by each concentration of PbTx-2 as determined from Figure 3c.

A.

KCl

B.

**KCl + 1 μM TTX**

C.

PbTx-2

D.

PbTx-2 + 1 μM TTX
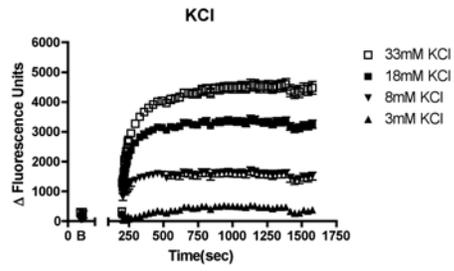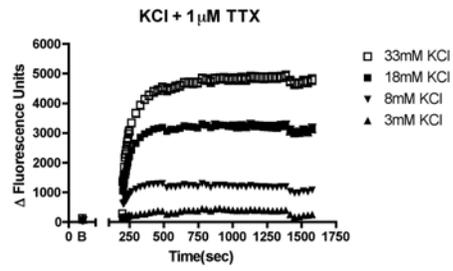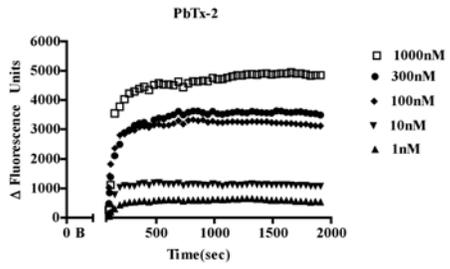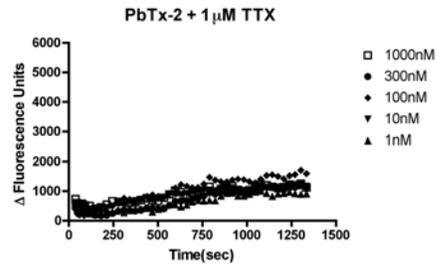
Figure 2.4. *The Effect of TTX, a VGSC antagonist, on PbTx-2-induced fluorescence output using DiBAC₄(3).* Neocortical neurons were treated with KCl or PbTx-2 in the presence and absence of TTX and fluorescence output of neocortical cells was monitored.
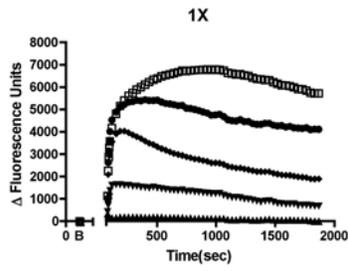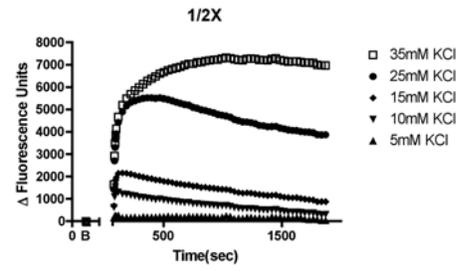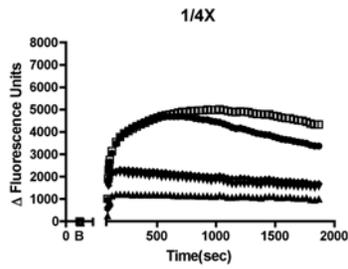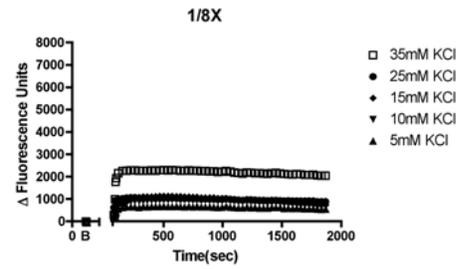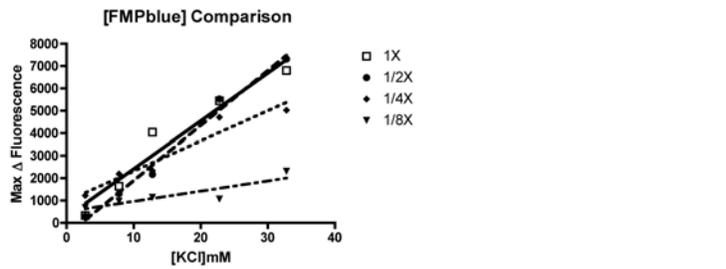
Figure 2.5. *A comparison of fluorescence output as a function of decreasing concentration of FMPblue dye.* In D, each point represents the maximum change in fluorescence induced by each indicated concentration of KCl.
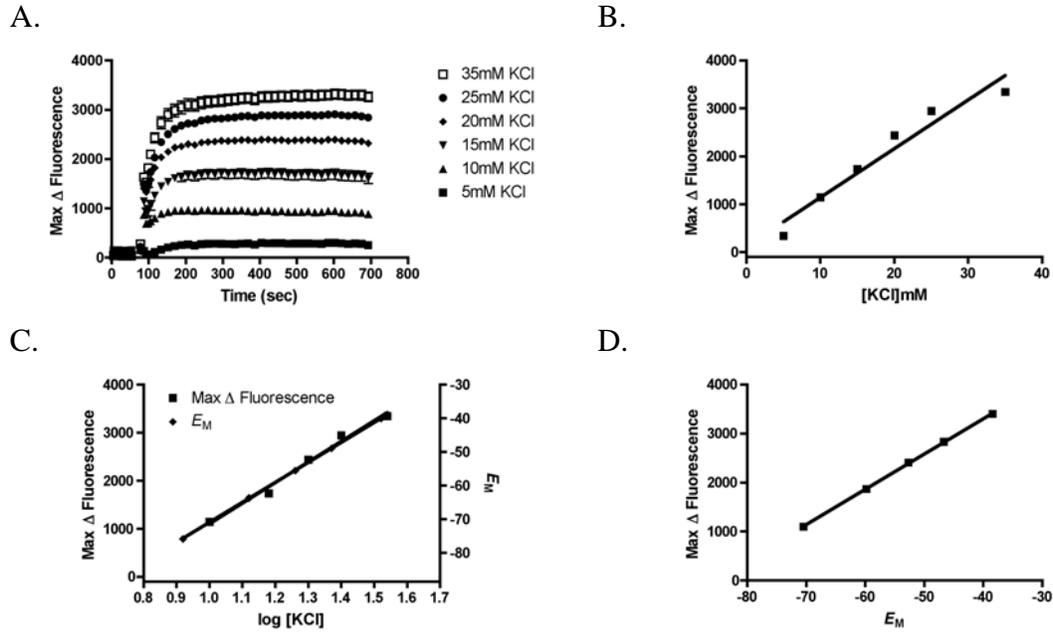
Figure 2.6. *KCl-induced changes in membrane potential are measured using FMPblue*.
In A, fluorescence output was monitored over time as a function of [KCl] and then
plotted as maximum change in fluorescence. In B, each point represents the maximum
change in fluorescence units induced by each concentration of KCl. In C, a comparison
of the regressions for log[KCl]-induced increments in fluorescence and calculated E_M
values derived from the modified Goldman equation were plotted. In D, the maximum
change in fluorescence is plotted against the membrane potential induced by each
concentration of KCl.

A.

B.

C.

D.
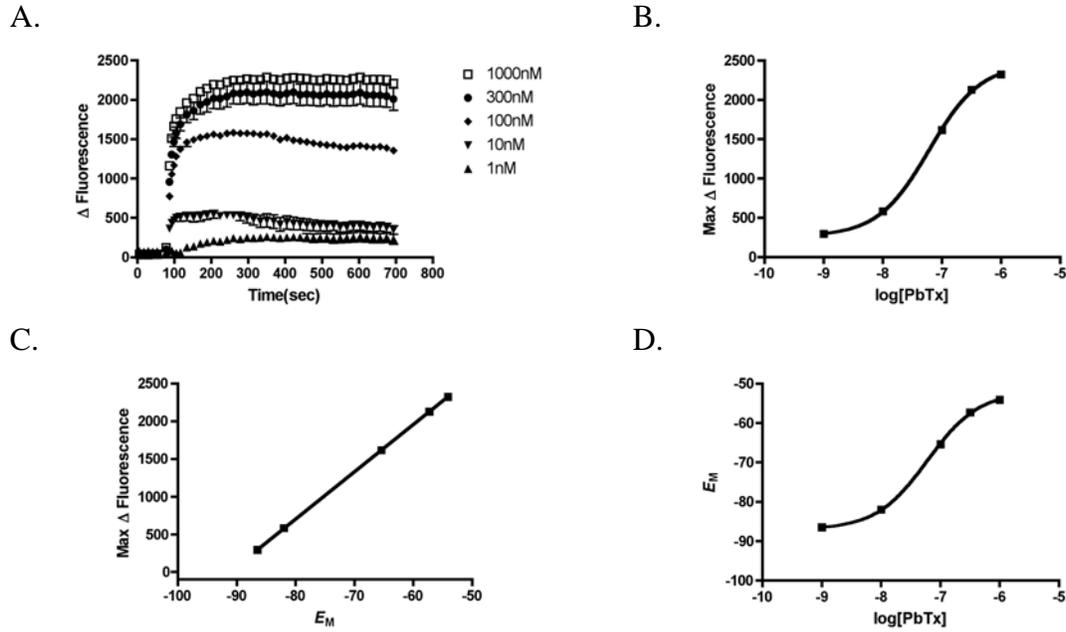
Figure 2.7. *PbTx-2-induced changes in membrane potential can be measured via comparison of fluorescence output with that achieved by an increase in extracellular K^+ levels using FMPblue.* In A, fluorescence output was monitored over time as a function of [PbTx-2] and then plotted as maximum change in fluorescence. In B, non-linear regression analysis of the maximum change in fluorescence for each concentration of PbTx-2 was plotted. In C, increments in fluorescent responses for each concentration of PbTx-2 were regressed to the corresponding values from KCl-induced changes in membrane potential reference plot. In D, each point represents the membrane potential induced by each concentration of PbTx-2 as determined from Figure 3c.
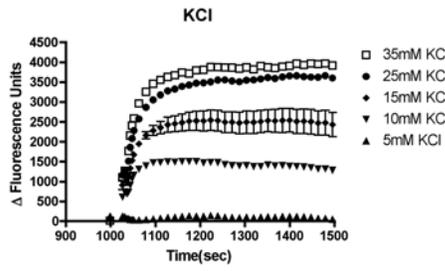
A.
B.
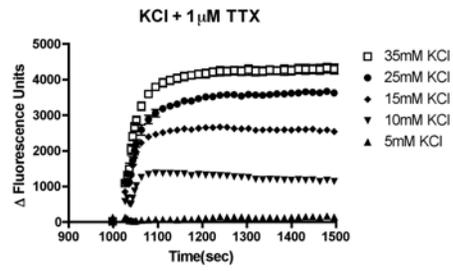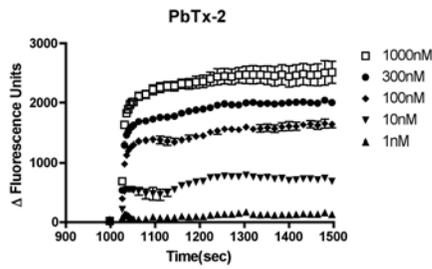
C.
D.
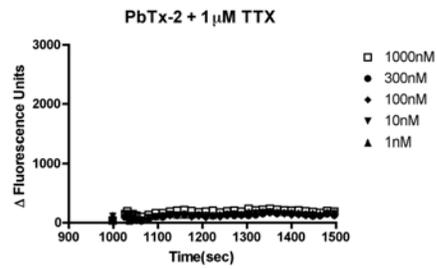
Figure 2.8. *The Effect of TTX, a VGSC antagonist, on PbTx-2-induced fluorescence output using FMPblue.* Neocortical neurons were treated with KCl or PbTx-2 in the presence and absence of TTX and fluorescence output of neocortical cells was monitored.
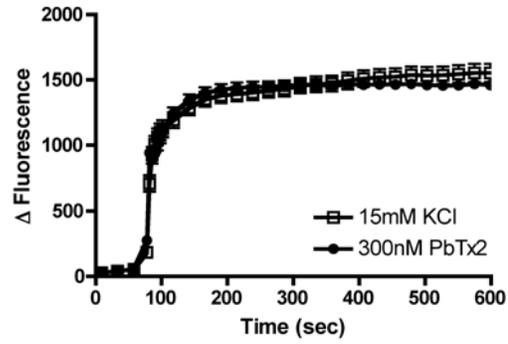
Figure 2.9. E*quivalent levels of membrane depolarization are induced by 300 nM PbTx-2 and 15 mM KCl in primary cultures neocortical cells.* Experiment was repeated three times with similar results.

A.

p-ERK1/2

ERK1/2

Ctrl   PbTx   KCl   KCl+TTX
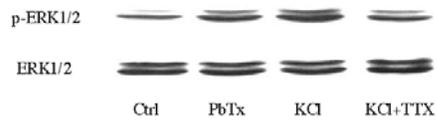
B.
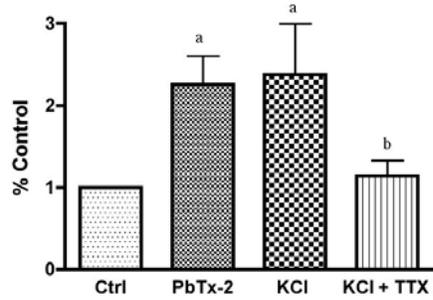
Figure 2.10. *ERK1/2 activation is dependent on Na$^+$ influx through VGSC.* In A, 300 nM PbTx-2 and 15 mM KCl produce similar levels of ERK1/2 phosphorylation; however, KCl-induced ERK1/2 phosphorylation is attenuated by TTX. In B, bands were analyzed using densitometry and plotted as a percent of control. [a]$p < 0.05$ when compared to control. [b]$p < 0.05$ when compared to KCl. Data shown represents the mean $\pm$ SEM of values (n=5).

Table 2.1. *Relationship between changes in DiBAC$_4$(3) fluorescence and calculated E_M values in response to various concentrations of K^+ and PbTx-2*

[PbTx-2] (nM)	Max Δ Fluorescence (rfu)	E_M (mV)	Equivalent [KCl] (mM)
1	749	-93.4	4
10	1220	-88.5	5
100	3235	-67.7	11
300	4242	-57.3	16
1000	4745	-52	20

Table 2.2. *Relationship between changes in FMPblue fluorescence and calculated E_M values in response to various concentrations of K^+ and PbTx-2*

[PbTx-2] (nM)	Max Δ Fluorescence (rfu)	E_M (mV)	Equivalent KCl (mM)
1	295	-86.5	5
10	583	-82	6
100	1616	-65.4	12
300	2129	-57.3	16
1000	2324	-54.1	19

CHAPTER 3

BREVETOXIN-INDUCED UPREGULATION OF NMDA RECEPTOR FUNCTION IS

REGULATED BY Src TYROSINE KINASE

ABSTRACT

Brevetoxins (PbTx1-10) are produced by the dinoflagellate *Karenia brevis* and have been implicated in thousands of marine animal mortalities and human exposures each year. These exposures have been linked to periodic 'red tide' events that result from explosive growth of the algae and have been found to occur in the Gulf of Mexico and along the coasts of New Zealand and Japan. Brevetoxins bind to and augment voltage-gated sodium channels (VGSC) in the brain producing repetitive action potentials that ultimately compromise the viability of the neuron. PbTx-induced neurotoxicity has been found to be mediated almost entirely by Ca^{2+} entering through *N*-methyl-D-aspartate receptors (NMDAR) as a consequence of PbTx-induced upregulation of VGSCs. It has been suggested that this upregulation may be attributed to the depolarizing influence of PbTx as a consequence of VGSC activation and/or to its activation of mechanisms leading to phosphorylation of NMDARs. Inasmuch as NMDAR phosphorylation has been documented to augment receptor function, we examined the ability of brevetoxin to induce NMDAR phosphorylation through the non-receptor tyrosine kinase, Src. We found that PP2, an inhibitor of Src, completely abolished PbTx-induced NMDAR phosphorylation indicating that Src is involved in NMDAR upregulation.

INTRODUCTION

Brevetoxins are potent, lipophilic neurotoxins produced by *Karenia brevis*, a dinoflagellate responsible for causing periodic "red tide" events that occur in the Gulf of Mexico and off the coasts of New Zealand and Japan [3,13]. These 'red tide' events result from explosive growth of the alga where blooms become easily lysed by beating currents releasing brevetoxin into the surrounding water and causing a significant increase in toxin concentration.

52

Brevetoxin may then undergo bubble-mediated transport to the surface where it becomes incorporated into marine aerosol [22].

Brevetoxin exposure has been implicated in numerous epizootic events including an unprecedented 1996 episode that occurred off the coast of Florida and involved the death of 149 manatees. Gross, histologic, and immunohistochemical analysis suggested that cells became programmed to cell death subsequent to the accumulation of brevetoxin in the body which eventually led to the release of inflammatory cytokines [6]. Humans may become exposed through a variety of routes including the skin, inhalation, and ingestion. Exposure to marine aerosol has been found to cause respiratory and conjunctiva irritation, bronchoconstriction, dizziness, and skin rashes [23]. Consumption of contaminated shellfish can lead to Neurotoxic Shellfish Poisoning, a syndrome encompassing gastroenteritis and neurological sequelae such as paresthesia, reversal of hot and cold temperature sensations, myalgia, vertigo, ataxia, and under extreme circumstances, seizures and coma [10,20].

Brevetoxins bind to voltage-gated sodium channels (VGSC) in the brain and periphery altering channel kinetics by causing an inhibition of the channel's fast inactivation gating mechanism, a shift of activation to more negative membrane potentials, and an increase in mean channel open time [14]. These effects generate the continuous propagation of action potentials effecting the excitability of nerve, muscle, and cardiac tissue [28]. Accumulation in the brain has been well documented to reach levels in which these effects are sufficient to alter CNS function [7]. Efforts have since been made to characterize these alterations in an attempt to fully elucidate the actions behind PbTx-induced neurotoxicity.

Recent efforts have focused on the ability of PbTx to induce effects similar to excitotoxicity, a phenomenon first coined by Olney, where a build-up of glutamate in the

synapse results in the overactivation of glutamate receptors and subsequent cytotoxicity [21,24,27]. These excitotoxic events have been found to be mediated by NMDARs inasmuch as Ca^{2+} entry through any other route fails to produce the same cytotoxic results as that which enters through NMDARs [15]. Furthermore, increasing intracellular Ca^{2+} levels alone fails to produce the same results [17]. Possible explanations include the "source-specificity" hypothesis, where specific Ca^{2+}-induced pathways are located close to the intracellular region of the NMDAR channel opening to allow for the following effects to be exclusively for NMDAR Ca^{2+} entry, and the idea that Ca^{2+} entry through the NMDAR has privileged access to the mitochondria [2,26,27].

Brevetoxin parallels these excitotoxic effects inasmuch as its binding to VGSCs manifests repetitive neuronal discharges causing the buildup of glutamate in the synapse ending in neurotoxicity [4,12]. Previous findings have reported that the NMDAR is most efficacious in increasing PbTx-induced Ca^{2+} influx and that PbTx-treated cells are more vulnerable to Ca^{2+} entering through the NMDAR than through any other route [5,8]. Furthermore, antagonism of NMDAR results in a reduction of PbTx-induced excitotoxicity [4]. These results indicate that PbTx-induced neurotoxicity is mediated entirely by NMDARs activated secondarily as a consequence of PbTx-induced stimulation of excitatory amino acid release [4]. However, PbTx may represent a more potent inducer of excitotoxicity than previously understood inducers inasmuch as the level of glutamate released into the synapse seems to be at levels which under normal circumstances would produce only modest neurotoxicity yet causes substantial changes in neuronal response associated with excitotoxic events [5]. This phenomenon has been proposed to be linked to the augmentation of NMDARs due to the depolarizing influence of PbTx activation of VGSCs and/or by the NMDAR modulatory protein Src tyrosine kinase [5,9].

Previously, we found that depolarization and subsequent removal of the voltage-dependent Mg^{2+} block do not result in the activation of molecules downstream of the NMDAR alone, but rather it is the increment in $[Na^+]_i$ that is required for their activation. Therefore, the ability of Na^+ to augment NMDARs appears to be involved in PbTx-2-induced neurotoxicity. To investigate a possible role for Src in PbTx-2-induced NMDAR upregulation, we used the Src tyrosine kinase inhibitor, PP2. Evidence suggests that upon Src activation, NMDAR activity is enhanced thereby boosting the entry of Ca^{2+} and triggering various downstream signaling cascades involved in such processes as neuronal growth and/or degeneration [25]. Here, we found that Src is responsible for PbTx-induced NMDAR phosphorylation and therefore appears to be mediating its excitotoxic effects.

MATERIALS AND METHODS

Neocortical Neuron Culture: Primary cell cultures of neocortical neurons were obtained from Swiss-Webster mice on embryonic day 16. Embryos were extracted following euthanasia via CO_2 asphyxiation and their neocortices were collected. Isolated neocortices were then removed of their meninges, minced by trituration using a Pasteur pipette, and treated with trypsin for 25 minutes at 37ºC. The cells were further dissociated via two successive trituration and sedimentation steps in isolation buffer containing soybean trypsin inhibitor and DNase. The cells underwent another centrifugation step and were resuspended in a neuron-plating medium containing Eagle's minimal essential medium with Earle's salt (MEM), along with 2 mM L-glutamine, 10% fetal bovine serum, 10% horse serum, 100 I.U./ml penicillin and 0.10 mg/ml streptomycin, pH=7.4. Cells were plated onto poly-L-lysine treated, 96 (9 mm) well, black, clear-bottomed culture plates at a density of 1 X 10^6 cells/well. Plates were incubated at 37 ºC

with 5% CO2 and 95% humidity. On day 2, post-plating, cells were treated with cytosine

arabinoside (10 μM) to prevent proliferation of non-neuronal cells. The culture media was

changed both on days 5, 8, and 11 using a serum-free growth medium containing 1X Neurobasal

medium supplemented with B-27 (Invitrogen), 100 I.U./ml penicillin, 0.10 mg/ml streptomycin,

and 0.2 mM L-glutamine. Cultures were used in experiments between 8-11 days *in vitro*. All

animal use protocols were approved by the Institutional Animal Care and Use Committee

(IACUC).

Membrane Potential Assay Kit Fluorescence Monitoring: Cells were removed of their

media and 100 μl of Locke's buffer was added to each well. Dye concentrations were made up

at 2X the desired concentration and 100 μl was added to the set wells. Cells were then incubated

at room temperature for 30 mins. All drug solutions were made up at 11X the final desired

concentration and 20 μl was added to each well. Fluorescence was measured using a

Fluorometric Imaging Plate Reader (FLIPR, Molecular Devices, Sunnyvale, CA) and a #2 filter

(540-590 nM bandpass). Neurons were excited to 530 nm and emission was measured within

550-565 nm. Exposure length (~0.7 sec) and laser power (~0.1 W) were adjusted to provide an

average baseline fluorescence of 7,000-10,000 rfu. Prior to each experiment, baseline

fluorescence was recorded to ensure normality across the plate.

Drug Treatment: Cells were washed three times with Locke's buffer and then allowed to

equilibrate in Locke's for 15 min. Any inhibitors were added during the equilibration period as

well. After this period, cultures were treated with the indicated drugs diluted in Locke's buffer

and incubated at 37°C for specified times. Cultures were then transferred to an ice slurry to

terminate treatment. After washing with ice cold PBS, cells were harvested in ice cold lysis

buffer containing 20 mM Tris, 150 mM NaCl, 1 mM EDTA, 1 mM EGTA, 1% Triton X-100,

2.5 mM sodium pyrophosphate, 1 mM sodium orthovanadate, 1 µg/ml leupeptin, and 1mM

PMSF just prior to use and incubated for 10 min at 4°C. Cell lysates then underwent sonification

and were centrifuged at 15,000 rpm for 10 min at 4°C.

Immunoprecipitation: Bradford analysis was performed on all samples to produce a final

sample solution of 1 µg of cell lysate/µl lysis buffer. Antibody was added at 1 µl/µg of cell

lysate and incubated overnight at 4°C. 20 µl of a protein A sepharose bead slurry was then

added and incubated for 2 hrs at 4°C. Samples were centrifuged for 30 sec followed by three

washes with subsequent centrifugation. The supernatant was set aside and 20 µl of 3X SDS

loading buffer was added to each sample resin to prepare for gel loading. Immunoprecipitation

supernatant was used as a negative control by adding an equal amount of 2X SDS loading buffer.

Correct bands were identified using several techniques including preabsorption,

immunoprecipitation of the supernatant, and running of markers.

Western Blotting: Protein samples were boiled for 5 min and then loaded onto a SDS-

PAGE gel. Gels were then transferred to a nitrocellulose membrane via electroblotting and

membranes were blocked in TBST (20 mM Tris, 150 mM NaCl, 0.1% Tween 20) with 5%

nonfat dry milk (TBST-MLK) for 1hr at room temperature. After washing four times in TBST,

membranes were incubated overnight at 4°C with constant rocking in a TBST and 5% bovine

serum albumin solution containing the appropriate dilution of primary antibody. Washing was

repeated with TBST followed by incubation in TBST-MLK containing secondary antibody for

one hour at room temperature. Blots were then washed four times in TBST and treated with

ECL plus for 4 min. Exposure was carried out on Kodak hyperfilm and film was developed.

Membranes could be stripped with stripping buffer (63 mM Tris base, 70 mM SDS, 0.0007% 2-

mercaptoethanol, pH=6.8) and reblotted for further use.

Materials: Trypsin, penicillin, streptomycin, heat-inactivated fetal bovine serum, horse serum and soybean trypsin inhibitor were obtained from Atlanta Biologicals (Norcross, GA). Minimum essential medium (MEM), Deoxyribonuclease (DNase), poly-L-lysine, cytosine arabinoside, Protein A Sepharose, anti-rabbit and anti-mouse IgG were purchased from Sigma (St. Louis, MO). Neurobasal and B-27 Supplement were purchased from Invitrogen Corporation (Carlsbad, CA). Tetrodotoxin (TTX) and Brevetoxin-2 (PbTx-2) were purchased from Tocris Cookson, Inc. (Ellisville, MO). Anti-p44/42 and phospho-p44/42 antibodies were purchased from Cell Signaling Technology (Beverly, MA), anti-phosphotyrosine (anti-phospoTyr) was purchased from BD Transduction Laboratories (San Diego, CA), anti-NR2Bphosphotyrosine (anti-NR2BphosphoTyr) was purchased from Chemicon (Temecula, CA) and anti-NR2B was purchased from Upstate (Charlottesville, VA). 4-Amino-5-(4-chlorophenyl)-7-(t-butyl)pyrazolo[3,4-d]pyrimidine (PP2), 4-Amino-7-phenylpyrazol[3,4-d]pyrimidine (PP3), and monensin were purchased from Calbiochem (La Jolla, CA). ECL kit was purchased from Amersham Biosciences (Piscataway, NJ). FLIPR® Membrane Potential Assay Kit was purchased from Molecular Devices (Sunnyvale, CA).

Data Analysis: Western Blot densitometry data was obtained using AIS software® (Imaging Research, Inc.) and data analysis and curve fitting was completed using GraphPad Prism® (GraphPad Software, Inc., San Diego, CA).

RESULTS

Defining optimum conditions for PbTx-induced phosphorylation of NMDARs

In previous studies, PbTx-2 has been shown to cause an increase in the phosphorylation of the NMDAR NR2B subunit [9]. In previous studies, NR2B phosphorylation has been found

to be involved in the upregulation of NMDAR activity [30]. These findings suggest a mechanism of PbTx-2-induced upregulation of NMDAR activity by way of tyrosine phosphorylation. To explore this idea, we first developed optimum conditions for PbTx-2-induced NMDAR phosphorylation by combining data from both immunoprecipitation and immunoblotting techniques using anti-NR2B, anti-NR2BphosphoTyr, and a general anti-phosphoTyr. We saw a concentration-dependent increase in NR2B phosphorylation up to 100 nM PbTx-2. PbTx-2 at 100 nM produced a two-fold increase over control in NR2B phosphorylation (Fig. 3.1A, B). The phosphorylation status of the protein began to fall, however, when introduced to higher concentrations such as 300 nM and 1 μM PbTx-2. PbTx-2 induced only a 1/2-fold increase over control at a concentration of 300 nM, while1 μM PbTx-2 failed to increase NR2B phosphorylation above control.

Using 100 nM PbTx-2, a time-response was then performed to determine the time required for optimum phosphorylation of the NMDAR. Results found that 100 nM PbTx-2 produced a steep rise in NR2B phosphorylation to that just above a two-fold increase within 15 min. After 15 min of exposure, PbTx-induced phosphorylation began to fall with 30 min of exposure producing only a one-fold increase above control (Fig. 3.2A, B). These data suggest optimum PbTx-induced NMDAR phosphorylation to occur during 15 min of exposure to 100 nM PbTx-2.

Src protein kinase is required for PbTx-2 induced phosphorylation of the NMDAR NR2B subunit.

Src is a protein kinase that is regulated by multiple pathways and has been found to participate in the regulation of NMDAR function through tyrosine phosphorylation [25]. Furthermore, it has been proposed that Src may act synergistically with Na^+ in the regulation of

NMDAR function and therefore is worthy of exploring in PbTx-induced augmentation of

NMDARs [31]. Previously, PbTx has been shown to increase tyrosine phosphorylation of the

NMDAR NR2B subunit and PbTx-induced Ca^{2+} influx through the channel has been reported to

be dependent on Src [9]. Here, we added the Src kinase inhibitor, PP2, to neocortical neurons

treated with 100 nM PbTx-2 to assess the involvement of Src in PbTx-induced NR2B

phosphorylation. We found that while PbTx-2-induced NR2B phosphorylation levels increased

to two-fold of control, PP2 (1 µM) completely eliminated this effect maintaining

phosphorylation levels near control. On the other hand, PP3 (1 µM), an inactive congener of

PP2, failed to completely attenuate PbTx-induced NR2B phosphorylation (Fig. 3.3A, B). This

data suggests that Src is required for PbTx-induced phosphorylation of the NMDAR NR2B

subunit.

DISCUSSION

　　　Src, a member of the Src family kinases (SFKs), is a protein tyrosine kinase that is highly

expressed in the CNS and abundant in neurons [25]. It is involved in such functions as the

regulation of ion channel activity and synaptic transmission [25]. Recent studies have focused

on its ability to regulate the NMDAR through phosphorylation of the NR2B subunit. Src-

mediated phosphorylation of this subunit has been found to cause channel upregulation thereby

initiating various synaptic signaling events and protein-protein interactions implicated in

learning, memory processing, pain perception, and multiple human disorders [1,18,25,29].

Recently, PbTx-induced NMDAR upregulation has been suggested to be mediated by

phosphorylation of the NR2B subunit while as PbTx was found to increase NMDAR tyrosine

phosphorylation and Src was found to be required for PbTx-induced Ca^{2+} influx through the

NMDAR [9]. To further evaluate the possible role of Src in PbTx-induced NMDAR phosphorylation, we used the Src family kinase inhibitor PP2. We found that PP2 significantly decreased PbTx-induced tyrosine phosphorylation of the NMDAR. It seems likely then that PbTx-2-induced augmentation of the NMDAR is at least partly regulated by Src kinase. Src phosphorylation of the NMDAR has been reported to participate in the recruitment of internalized NMDARs to the membrane leading to an increase in Ca^{2+} flux and subsequent neuronal cell death [25]. This function may help to explain previous observations of PbTx-induced differential regulation of ERK1/2 signaling inasmuch as the recruitment of internalized NMDARs to the membrane via Src-mediated NMDAR phosphorylation may result in the initiation of different cell signaling pathways ultimately resulting in those mechanisms associated with apoptosis as opposed to cell survival [9]. Further exploration is required to define this role for Src in PbTx-induced neurotoxicity.

Previously, we reported that Na^+ appears to be involved in NMDAR upregulation as well. The degree of augmentation induced by either PbTx-induced phosphorylation or an increase in Na^+ has yet to be defined. It may be that these two mechanisms work synergistically to mediate receptor upregulation. Previous studies indicate that Zn^{2+}-induced upregulation of NMDAR function is mediated by both an increase in Na^+ and Src activation [16,19]. Other studies have found that Src not only increases NMDAR function by phosphorylation but also acts to sensitize the channels to potentiation by Na^+ [30]. These findings suggest that PbTx, a potent allosteric activator of VGSCs, follows a similar mechanism where both Src kinase and Na^+ work synergistically to augment NMDAR function.

NMDARs are vital in many important physiological functions including synaptic plasticity and neuronal survival. These receptors, however, demonstrate a kind of Jekyll and

Hyde behavior as their overactivation can lead to cell death [12]. This overactivation of NMDARs has been implicated in many conditions that lead to neuronal death including stroke, seizure, and mechanical trauma and is thought to contribute to various neurodegenerative disorders such as Huntington's disease, HIV-associated dementia and Alzheimer's disease [11]. By uncovering the mechanisms behind PbTx-induced NMDAR regulation, we may begin to characterize not only the mechanisms behind PbTx-induced neurotoxicity but also those behind related neurological conditions.

REFERENCES

[1]   Ali, D.W. and Salter, M.W., NMDA receptor regulation by Src kinase signalling in excitatory synaptic transmission and plasticity, *Curr Opin Neurobiol*, 11 (2001) 336-42.

[2]   Arundine, M. and Tymianski, M., Molecular mechanisms of calcium-dependent neurodegeneration in excitotoxicity, *Cell Calcium*, 34 (2003) 325-37.

[3]   Baden, D.G., and David J. Adams, Brevetoxins: Chemistry, Mechanism of Action, and Methods of Detection. In L.M. Botana (Ed.), *Seafood and Freshwater Toxins. Pharmacology, Physiology, and Detection*, Marcel Dekker, Inc., New York, Basal, 2000, pp. 505-532.

[4]   Berman, F.W. and Murray, T.F., Brevetoxins cause acute excitotoxicity in primary cultures of rat cerebellar granule neurons, *J Pharmacol Exp Ther*, 290 (1999) 439-44.

[5]   Berman, F.W. and Murray, T.F., Brevetoxin-induced autocrine excitotoxicity is associated with manifold routes of Ca^{2+} influx, *J Neurochem*, 74 (2000) 1443-51.

[6]   Bossart, G.D., Baden, D.G., Ewing, R.Y., Roberts, B. and Wright, S.D., Brevetoxicosis in manatees (Trichechus manatus latirostris) from the 1996 epizootic: gross, histologic, and immunohistochemical features, *Toxicol Pathol*, 26 (1998) 276-82.

[7]   Cattet, M. and Geraci, J.R., Distribution and elimination of ingested brevetoxin (PbTx-3) in rats, *Toxicon*, 31 (1993) 1483-6.

[8]   Dravid, S.M., Baden, D.G. and Murray, T.F., Brevetoxin activation of voltage-gated sodium channels regulates Ca^{2+} dynamics and ERK1/2 phosphorylation in murine neocortical neurons, *J Neurochem*, 89 (2004) 739-49.

[9]   Dravid, S.M., Baden, D.G. and Murray, T.F., Brevetoxin augments NMDA receptor signaling in murine neocortical neurons, *Brain Res*, 1031 (2005) 30-8.

[10]   Ellis, S., Introduction to symposium- Brevetoxins: chemistry and pharmacology of 'red tide' toxins from *Ptychodiscus brevis* (formerly *Gymnodinium breve*), *Toxicon*, 23 (1985) 469-172.

[11]   Hardingham, G.E. and Bading, H., The Yin and Yang of NMDA receptor signalling, *Trends Neurosci*, 26 (2003) 81-9.

[12]   Huang, J.M., Wu, C.H. and Baden, D.G., Depolarizing action of a red-tide dinoflagellate brevetoxin on axonal membranes, *J Pharmacol Exp Ther*, 229 (1984) 615-21.

[13]   Ishida, H., Muramatsu, N., Nukaya, H., Kosuge, T. and Tsuji, K., Study on neurotoxic shellfish poisoning involving the oyster, Crassostrea gigas, in New Zealand, *Toxicon*, 34 (1996) 1050-3.

[14]   Jeglitsch, G., Rein, K., Baden, D.G. and Adams, D.J., Brevetoxin-3 (PbTx-3) and its derivatives modulate single tetrodotoxin-sensitive sodium channels in rat sensory neurons, *J Pharmacol Exp Ther*, 284 (1998) 516-25.

[15] Kato, K. and Murota, S., NMDA receptor stimulation in the absence of extracellular Ca^{2+} potentiates Ca^{2+} influx-dependent cell death system, *Brain Research*, 1035 (2005) 177-187.

[16] Kim, T.W., Hwang, J.J., Yun, S.H., Jung, M.W. and Koh, J.Y., Augmentation by zinc of NMDA receptor-mediated synaptic responses in CA1 of rat hippocampal slices: mediation by Src family tyrosine kinases., *Synapse 46* (2002) 49-56.

[17] Li, J., Kato, K., Ikeda, J., Morita, I. and Murota, S., A narrow window for rescuing cells by the inhibition of calcium influx and the importance of influx route in rat cortical neuronal cell death induced by glutamate, *Neurosci Lett*, 304 (2001) 29-32.

[18] Loftis, J.M. and Janowsky, A., The N-methyl-D-aspartate receptor subunit NR2B: localization, functional properties, regulation, and clinical implications, *Pharmacol Ther*, 97 (2003) 55-85.

[19] Manzerra, P., Behrens, M.M., Canzoniero, L.M., Wang, X.Q., Heidinger, V., Ichinose, T., Yu, S.P. and Choi, D.W., Zinc induces a Src family kinase-mediated up-regulation of NMDA receptor activity and excitotoxicity, *Proc Natl Acad Sci U S A*, 98 (2001) 11055-11061.

[20] Morris, M.D., Campbell, D.S., Taylor, T.J. and Freeman, J.I., Clinical and Epidemiological Features of Neurotoxic Shellfish Poisoning in North Carolina, *American Journal of Public Health*, 81 (1991) 471-474.

[21] Olney, J.W., Brain lesions, obesity, and other disturbances in mice treated with monosodium glutamate, *Science*, 164 (1969) 719-21.

[22]   Pierce, R.H., Henry, M.S., Blum, P.C., Lyons, J., Cheng, Y.S., Yazzie, D. and Zhou, Y.,
        Brevetoxin concentrations in marine aerosol: human exposure levels during a Karenia
        brevis harmful algal bloom, *Bull Environ Contam Toxicol*, 70 (2003) 161-5.

[23]   Richards, I.S., Kulkarni, A.P., Brooks, S.M. and Pierce, R., Florida red-tide toxins
        (brevetoxins) produce depolarization of airway smooth muscle, *Toxicon*, 28 (1990) 1105-
        11.

[24]   Rothman, S.M. and Olney, J.W., Excitotoxicity and the NMDA receptor--still lethal after
        eight years, *Trends Neurosci*, 18 (1995) 57-8.

[25]   Salter, M.W., Src, N-methyl-D-aspartate (NMDA) receptors, and synaptic plasticity,
        Biochem Pharmacol, 56 (1998) 789-98.

[26]   Sattler, R., Charlton, M.P., Hafner, M. and Tymianski, M., Distinct influx pathways, not
        calcium load, determine neuronal vulnerability to calcium neurotoxicity, *J Neurochem*,
        71 (1998) 2349-64.

[27]   Sattler, R. and Tymianski, M., Molecular mechanisms of calcium-dependent
        excitotoxicity, *J Mol Med*, 78 (2000) 3-13.

[28]   Wang, S.Y. and Wang, G.K., Voltage-gated sodium channels as primary targets of
        diverse lipid-soluble neurotoxins, *Cell Signal*, 15 (2003) 151-9.

[29]   Yu, X.M., Askalan, R., Keil, G.J., 2nd and Salter, M.W., NMDA channel regulation by
        channel-associated protein tyrosine kinase Src, *Science*, 275 (1997) 674-8.

[30]   Yu, X.M. and Salter, M.W., Gain control of NMDA-receptor currents by intracellular
        sodium, *Nature*, 396 (1998) 469-74.

[31]   Yu, X.M. and Salter, M.W., Src, a molecular switch governing gain control of synaptic transmission mediated by N-methyl-D-aspartate receptors, *Proc Natl Acad Sci U S A*, 96 (1999) 7697-704.

A.
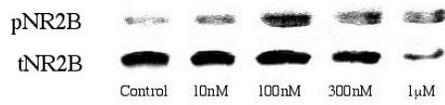
B.
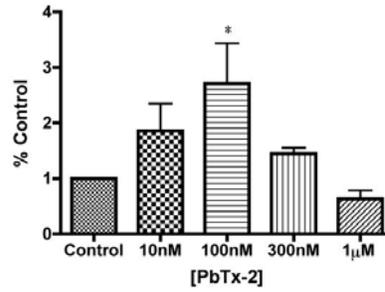
Figure 3.1. *PbTx-2 induces optimum phosphorylation of the NR2B subunit at a*

concentration of 100 nM. Experiment was repeated three times with similar results. In B,

bands were analyzed using densitometry and blotted as a percent of control. Data shown

represents the mean ± SEM of values (n=3). *p< 0.05 when compared to control.

A.
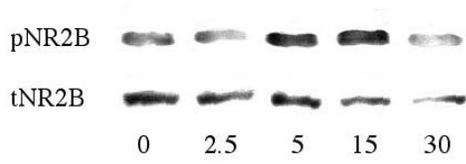
B.
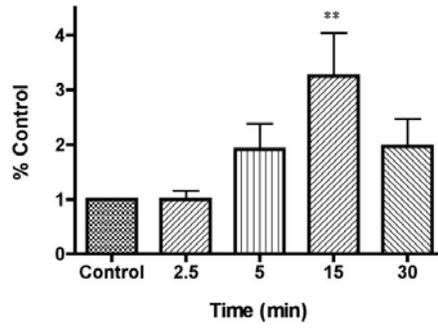
Figure 3.2. *Optimum phosphorylation of the NR2B subunit occurs by exposing neocortical neurons in culture to 100 nM PbTx-2 for 15min.* In B, bands were analyzed using densitometry and plotted as a percent of control. Data shown represents the mean ± SEM of values (n=3). **$p < 0.01$ when compared to control.

A.

pNR2B				
tNR2B				
PbTx	−	+	+	+
PP2	−	−	+	−
PP3	−	−	−	+
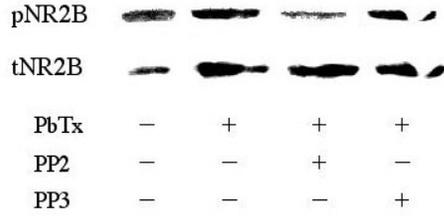
B.
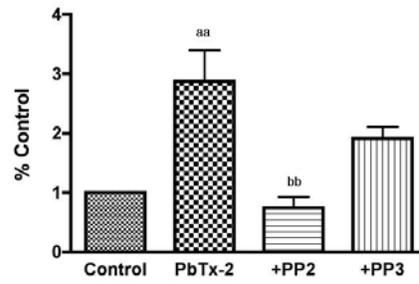
Figure 3.3. *PbTx-2 induced phosphorylation of NR2B is mediated by Src kinase.* In B, bands were analyzed using densitometry and plotted as a percent of control. Data shown represents the mean ± SEM of values (n=4). [aa]$p < 0.01$ when PbTx-2 was compared to control. [bb]$p < 0.01$ when PbTx-2+PP2 was compared to PbTx-2.

CHAPTER 4

SUMMARY AND CONCLUSIONS

Harmful algal blooms (HABs), such as *Karenia brevis*, are responsible for thousands of marine animal mortalities and human toxicities each year. They have been found to be increasing in frequency and severity and pose increasing risks to human health, natural resources and environmental quality in many U.S. coastal environments and worldwide [8]. Their economic impact alone results in annual losses of billions of dollars in income worldwide. Red tides, in particular, are associated with an estimated 100 tons of dead fish per day [9]. Thousands of human exposures occur each year through inhalation and ingestion of contaminated shellfish. Ingestion of contaminated shellfish results in a syndrome known as Neurotoxic Shellfish Poisoning which results in symptoms ranging from nausea and diarrhea to seizures and even coma.

Brevetoxins bind to neurotoxin site 5 of voltage-gated sodium channels (VGSCs) in neural tissue. This binding results in an augmentation of VGSC function causing a shift in the activation potential to more negative values, prolongation of mean channel open time and inhibition of channel inactivation. These effects may induce a state of repetitive action potentials. Brevetoxin-induced depolarization of cerebellar granule neurons in culture results in excessive glutamate release and overactivation of *N*-methyl-D-aspartate receptors (NMDAR) [4,6,15]. Due to their Ca^{2+} permeability, exaggerated activation of NMDARs leads to a massive influx of extracellular Ca^{2+} that initiates a cascade of events eventually leading to cell death [3,7]. These effects contribute to the phenomenon known as excitotoxicity. As first coined by Olney, an excitotoxic event is defined by the initiation of excessive excitatory amino acid release and subsequent overactivation of glutamate receptors [2,21,22]. The resulting Ca^{2+} overload ultimately leads to neuronal degeneration [2,21,22]. However, previous findings suggest that PbTx may represent a more potent inducer of excitotoxicity than previously understood inducers

inasmuch as the level of glutamate released into the synapse seems to be at levels which under normal circumstances would produce only modest neurotoxicity yet causes substantial changes in neuronal response associated with excitotoxic events [7]. This phenomenon has been proposed to be linked to the augmentation of NMDARs due to the depolarizing influence of PbTx activation of VGSCs and/or by the NMDAR modulatory protein Src tyrosine kinase [7,11].

There have been many studies on mechanisms that may contribute to the upregulation of NMDARs. In previous studies, Na^+ has been suggested not only to participate in the depolarization-mediated removal of the NMDAR Mg^{2+} blockade but to also more specifically play a role in NMDAR upregulation through interaction with the receptor. These studies have found that an increase in intracellular Na^+ causes an upregulation of NMDAR function [30,32]. PbTx-2 has been shown to augment NMDAR-mediated ERK2 activation and that this augmentation is not only dependent on Na^+ influx through VGSCs but also on the augmentation of Ca^{2+} influx through the NMDAR [10,11].

To distinguish between the role of depolarization and intracellular Na^+ in PbTx-2-induced NMDAR upregulation, a technique for measuring membrane depolarization was first developed. We compared the two membrane potential-sensitive fluorescent dyes $DiBAC_4(3)$ and FMPblue in neocortical neurons to optimize assay conditions for intact neurons and developed a method for measuring PbTx-2-induced depolarization. We found that $DiBAC_4(3)$ provides an optimum fluorescence signal in neocortical cells when used at 2.5 μM. FMPblue gave similar results inasmuch as it provides an optimum signal at one-half the manufacturer-suggested concentration, and can be utilized at concentrations as low as one-fourth that concentration with adequate fluorescence output. FMPblue provided an improvement in the fluorescence assay in that it was characterized by an increase in the signal to noise ratio. An added benefit of this dye

was its more rapid response times as compared to $DiBAC_4(3)$. These data with neurons correlate well with previous studies in which the two dyes were compared and indicate the use of membrane-potential sensitive fluorescent dyes as a practical and efficient method in detecting changes in membrane potential in primary cultures of neocortical neurons [5,12,27,28].

Brevetoxin has been shown to increase intracellular Na^+ concentrations through binding to neurotoxin site 5 on VGSCs [26]. Tetrodotoxin (TTX), an antagonist of VGSCs, inhibits both PbTx -induced Na^+ current in rat sensory neurons and the subsequent ERK1/2 activation in neocortical neurons [10,15]. In the results reported herein, TTX had no effect on the fluorescent signal produced by an elevation of extracellular K^+ whereas it inhibited the increment in fluorescent signal produced by brevetoxin in neocortical cells. These data agree with previous reports in which TTX prevented PbTx-induced depolarization while having no effect on potassium channels [14]. These findings support the notion that brevetoxin exerts its depolarizing influence through an alteration of VGSC gating properties.

To better quantify PbTx-2 modulation of neuronal excitability, we utilized extracellular K^+ as a reference for linking changes in fluorescence with membrane potential (E_M). This permitted quantification of PbTx-induced changes in neuronal E_M. Using this approach we found that 15 mM KCl and 300 nM PbTx-2 produced equivalent maximum changes in fluorescent emission and therefore represent concentrations that produce an equivalent E_M of approximately –60 mV. Using concentrations of PbTx and KCl that produce equivalent levels of depolarization, experiments with TTX were implemented to distinguish between depolarization per se versus Na^+ influx as essential for PbTx augmentation of NMDAR function.

To further assess the role of Na^+ in the upregulation of the NMDAR, we examined the effect of TTX on K^+-induced ERK1/2 activation using 15 mM KCl, a concentration

73

demonstrated to produce an equivalent level of depolarization as that induced by 300 nM PbTx-2. Previously, PbTx-2-induced ERK1/2 activation has been shown to be inhibited by TTX and thus mediated by VGSC activation [10]. In the current study, ERK1/2 activation induced by 15 mM KCl was inhibited by TTX as well. This data, in junction with our previous findings where KCl-induced depolarization was found to occur independent of Na^+ influx, demonstrates a separation between the effects of $[Na^+]_i$ and depolarization. These data suggest that depolarization and subsequent removal of the voltage-dependent Mg^{2+} block do not result in ERK1/2 activation alone, but rather it is the increment in $[Na^+]_i$ that is required for ERK1/2 activation. Therefore, the ability of Na^+ to augment NMDARs appears to be involved in PbTx-2-induced ERK1/2 activation.

Src, a member of the Src family kinases (SFKs), is a protein tyrosine kinase that is highly expressed in the CNS and abundant in neurons [24]. It is involved in such functions as the regulation of ion channel activity and synaptic transmission [24]. Recent studies have focused on its ability to regulate the NMDAR through phosphorylation of the NR2B subunit. Src-mediated phosphorylation of this subunit has been found to cause channel upregulation thereby initiating various synaptic signaling events and protein-protein interactions implicated in learning, memory processing, pain perception, and multiple human disorders [1,17,24,31]. Recently, PbTx-induced NMDAR upregulation has been suggested to be mediated by phosphorylation of the NR2B subunit while PbTx was found to increase NMDAR tyrosine phosphorylation and Src was found to be required for PbTx-induced Ca^{2+} influx through the NMDAR [11].

To further evaluate the possible role of Src in PbTx-induced NMDAR phosphorylation, we used the Src family kinase inhibitor PP2. We found that PP2 significantly decreased PbTx-

induced tyrosine phosphorylation of the NMDAR. It seems likely then that PbTx-2-induced augmentation of the NMDAR is at least partly regulated by Src kinase. Src phosphorylation of the NMDAR has been reported to participate in the recruitment of internalized NMDARs to the membrane leading to an increase in Ca^{2+} flux and subsequent neuronal cell death [25]. This function may help to explain previous observations of PbTx-induced differential regulation of ERK1/2 signaling inasmuch as the recruitment of internalized NMDARs to the membrane via Src-mediated NMDAR phosphorylation may result in the initiation of different cell signaling pathways ultimately resulting in those mechanisms associated with apoptosis as opposed to cell survival [9]. Further exploration is required to define this role for Src in PbTx-induced neurotoxicity.

The degree of augmentation induced by either PbTx-induced phosphorylation or an increase in Na^+ has yet to be defined. It may be that these two mechanisms work synergistically to mediate receptor upregulation. Previous studies indicate that Zn^{2+}-induced upregulation of NMDAR function is mediated by both an increase in Na^+ and Src activation [16,18]. Other studies have found that Src not only increases NMDAR function by phosphorylation but also acts to sensitize the channels to potentiation by Na^+ [32]. These findings suggest that PbTx, a potent allosteric activator of VGSCs, follows a similar mechanism where both Src kinase and Na^+ work synergistically to augment NMDAR function.

Experimental studies involving brevetoxin have thus far revealed a mechanism of action centered on major channels and pathways in the brain which have been found to be involved in such processes as learning and memory and cell growth, proliferation, and differentiation. These pathways have also been implicated in acute neuronal cell death associated with ischemia, brain insult, anoxia, hypoglycemia, seizure, and perinatal asphyxia as well as in pathological

conditions such as Huntington's disease, Brugada's syndrome, Hyperkalaemic periodic paralysis, HIV-associated dementia, Alzheimer's disease, Parkinson's disease, motor neuron disease, amyotrophic lateral sclerosis, epilepsy, chronic pain, stroke, and psychosis [13,19,20,23-25,29].

Brevetoxin exposures continue to be on the rise; fortunately, the pool of information on the toxin is growing as well. Much has been discovered about the structure of brevetoxin and how its interaction with VGSCs elicits a depolarization stimulus; however, there is still much to be elucidated about the downstream effects of brevetoxin exposure and how these effects on a cellular level lead to the symptoms associated with toxicity. These findings underscore the importance of further research on brevetoxin and the mechanisms behind its toxicity. This information will provide incite into treatments and prevention strategies not only for brevetoxin exposure situations but also for this overwhelming amount of associated conditions.

REFERENCES

[1]   Ali, D.W. and Salter, M.W., NMDA receptor regulation by Src kinase signalling in excitatory synaptic transmission and plasticity, *Curr Opin Neurobiol*, 11 (2001) 336-42.

[2]   Arundine, M. and Tymianski, M., Molecular mechanisms of calcium-dependent neurodegeneration in excitotoxicity, *Cell Calcium*, 34 (2003) 325-37.

[3]   Atlante, A., Calissano, P., Bobba, A., Giannattasio, S., Marra, E. and Passarella, S., Glutamate neurotoxicity, oxidative stress and mitochondria, *FEBS Lett*, 497 (2001) 1-5.

[4]   Baden, D.G., Brevetoxins: unique polyether dinoflagellate toxins, *Faseb J*, 3 (1989) 1807-17.

[5]   Baxter, D.F., Kirk, M., Garcia, A.F., Raimondi, A., Holmqvist, M.H., Flint, K.K., Bojanic, D., Distefano, P.S., Curtis, R. and Xie, Y., A novel membrane potential-

sensitive fluorescent dye improves cell-based assays for ion channels, *J Biomol Screen*, 7 (2002) 79-85.

[6]   Berman, F.W. and Murray, T.F., Brevetoxins cause acute excitotoxicity in primary cultures of rat cerebellar granule neurons, *J Pharmacol Exp Ther*, 290 (1999) 439-44.

[7]   Berman, F.W. and Murray, T.F., Brevetoxin-induced autocrine excitotoxicity is associated with manifold routes of Ca^{2+} influx, *J Neurochem*, 74 (2000) 1443-51.

[8]   Boesch, D.F., Anderson, D.M., Horner, R.A., Shumway, S.E., Tester, P.A. and Whitledge, T.E., Harmful Algal Blooms in Coastal Waters: Options for Prevention, Control and Mitigation. *An Assessment Conducted for The National Fish and Wildlife Foundation and The National Oceanic and Atmospheric Administration Coastal Ocean Program*, Center for Sponsored Coastal Ocean Research, Coastal Ocean Program, Chesapeake Research Consortium, Edgewater, Maryland 21037, 1997.

[9]   Catterall, W.A., From ionic currents to molecular mechanisms: the structure and function of voltage-gated sodium channels, *Neuron*, 26 (2000) 13-25.

[10]   Dravid, S.M., Baden, D.G. and Murray, T.F., Brevetoxin activation of voltage-gated sodium channels regulates Ca^{2+} dynamics and ERK1/2 phosphorylation in murine neocortical neurons, *J Neurochem*, 89 (2004) 739-49.

[11]   Dravid, S.M., Baden, D.G. and Murray, T.F., Brevetoxin augments NMDA receptor signaling in murine neocortical neurons, *Brain Res*, 1031 (2005) 30-8.

[12]   Gonzalez, J.E., Oades, K., Leychkis, Y., Harootunian, A. and Negulescu, P.A., Cell-based assays and instrumentation for screening ion-channel targets, *Drug Discovery Today*, 4 (1999) 431-439.

[13]   Hardingham, G.E. and Bading, H., The Yin and Yang of NMDA receptor signalling,
         Trends Neurosci, 26 (2003) 81-9.

[14]   Huang, J.M., Wu, C.H. and Baden, D.G., Depolarizing action of a red-tide dinoflagellate
         brevetoxin on axonal membranes, *J Pharmacol Exp Ther*, 229 (1984) 615-21.

[15]   Jeglitsch, G., Rein, K., Baden, D.G. and Adams, D.J., Brevetoxin-3 (PbTx-3) and its
         derivatives modulate single tetrodotoxin-sensitive sodium channels in rat sensory
         neurons, *J Pharmacol Exp Ther*, 284 (1998) 516-25.

[16]   Kim, T.W., Hwang, J.J., Yun, S.H., Jung, M.W. and Koh, J.Y., Augmentation by zinc of
         NMDA receptor-mediated synaptic responses in CA1 of rat hippocampal slices:
         mediation by Src family tyrosine kinases., *Synapse 46* (2002) 49-56.

[17]   Loftis, J.M. and Janowsky, A., The N-methyl-D-aspartate receptor subunit NR2B:
         localization, functional properties, regulation, and clinical implications, *Pharmacol Ther*,
         97 (2003) 55-85.

[18]   Manzerra, P., Behrens, M.M., Canzoniero, L.M., Wang, X.Q., Heidinger, V., Ichinose,
         T., Yu, S.P. and Choi, D.W., Zinc induces a Src family kinase-mediated up-regulation of
         NMDA receptor activity and excitotoxicity, *Proc Natl Acad Sci U S A*, 98 (2001) 11055-
         11061.

[19]   Meldrum, B.S., Glutamate as a neurotransmitter in the brain: review of physiology and
         pathology, *J Nutr*, 130 (2000) 1007S-15S.

[20]   Mori, H. and Mishina, M., Structure and function of the NMDA receptor channel,
         Neuropharmacology, 34 (1995) 1219-37.

[21]   Olney, J.W., Brain lesions, obesity, and other disturbances in mice treated with
         monosodium glutamate, *Science*, 164 (1969) 719-21.

[22]   Rothman, S.M. and Olney, J.W., Excitotoxicity and the NMDA receptor--still lethal after eight years, *Trends Neurosci*, 18 (1995) 57-8.

[23]   Said, S.I., Glutamate receptors and asthmatic airway disease, *Trends Pharmacol Sci*, 20 (1999) 132-4.

[24]   Salter, M.W., Src, N-methyl-D-aspartate (NMDA) receptors, and synaptic plasticity, *Biochem Pharmacol*, 56 (1998) 789-98.

[25]   Salter, M.W. and Kalia, L.V., Src kinases: a hub for NMDA receptor regulation, *Nat Rev Neurosci*, 5 (2004) 317-28.

[26]   Wang, S.Y. and Wang, G.K., Voltage-gated sodium channels as primary targets of diverse lipid-soluble neurotoxins, *Cell Signal*, 15 (2003) 151-9.

[27]   Whiteaker, K.L., Gopalakrishnan, S.M., Groebe, D., Shieh, C.C., Warrior, U., Burns, D.J., Coghlan, M.J., Scott, V.E. and Gopalakrishnan, M., Validation of FLIPR membrane potential dye for high throughput screening of potassium channel modulators, *J Biomol Screen*, 6 (2001) 305-12.

[28]   Wolff, C., Fuks, B. and Chatelain, P., Comparative study of membrane potential-sensitive fluorescent probes and their use in ion channel screening assays, *J Biomol Screen*, 8 (2003) 533-43.

[29]   Wood, J.N. and Baker, M., Voltage-gated sodium channels, *Curr Opin Pharmacol*, 1 (2001) 17-21.

[30]   Xin, W.K., Kwan, C.L., Zhao, X.H., Xu, J., Ellen, R.P., McCulloch, C.A. and Yu, X.M., A functional interaction of sodium and calcium in the regulation of NMDA receptor activity by remote NMDA receptors, *J Neurosci*, 25 (2005) 139-48.

[31]   Yu, X.M., Askalan, R., Keil, G.J., 2nd and Salter, M.W., NMDA channel regulation by channel-associated protein tyrosine kinase Src, *Science*, 275 (1997) 674-8.

[32]   Yu, X.M. and Salter, M.W., Gain control of NMDA-receptor currents by intracellular sodium, *Nature*, 396 (1998) 469-74.